A risk-constrained time-dependent cash-in-transit routing problem in multigraph under uncertainty

Hamid Tikani[1], Mostafa Setak[2], Emrah Demir[3]

1. First author: Department of Industrial Engineering, K. N. Toosi University of Technology, Tehran, Iran;
Ph.D candidate of Industrial Engineering; E-mail: hamid.tikani@email.kntu.ac.ir

2. **Corresponding author:** Department of Industrial Engineering, K. N. Toosi University of Technology, Tehran, Iran;
Associate professor; E-mail: setak@kntu.ac.ir ; Tel: (+9821)84063373

3. PARC Institute of Manufacturing, Logistics and Inventory, Cardiff Business School, Cardiff University, Cardiff, United Kingdom;
Associate professor; E-mail: demire@cardiff.ac.uk; Tel: +44 (0)29 2087 0971.

A risk-constrained time-dependent cash-in-transit routing problem in multigraph under uncertainty

Hamid Tikani[1], Mostafa Setak[1], Emrah Demir[2]

1. Department of Industrial Engineering, K. N. Toosi University of Technology, Tehran, Iran
2. PARC Institute of Manufacturing, Logistics and Inventory, Cardiff Business School, Cardiff University, Cardiff, United Kingdom

Abstract:

The Cash-in-Transit (CIT) deals with the transportation of banknotes, coins, and other valuable items. Due to the high-value density of these products, incorporating security strategies in the carrier operations is crucial. This paper proposes new CIT models involving deterministic and stochastic time-varying traffic congestion. Since risk exposure of a vehicle is proportional to the time-dependent travel time, a new formula is introduced to measure the risk of traveling. Moreover, this study covers one of the important weaknesses of previous CIT routing models by investigating the problem in multigraph networks. Multigraph representation maintains a set of non-dominated parallel arcs, which are differentiated by two attributes including travel time and robbery risk. Considering maximum allowable time duration together with a risk threshold yields to design a more balanced routing scheme. Multi-attribute parallel arcs in a stochastic time-dependent network bring high computational challenges. Herein, we introduce efficient algorithms including a novel flexible restricted Dynamic Programming and a self-adaptive caching Genetic Algorithm. The proposed algorithms are tested on both a real case study in Isfahan metropolis and generated instances. Ultimately, sensitivity analyses are conducted to assess the importance of the use of multigraph networks in the CIT and to provide significant managerial insights for administrators and practitioners.

Keywords: *Routing, cash-in-transit, multigraph network, time dependency, security risk*

1. Introduction

Globally, cash continues to be a widely used payment instrument for transactions. This instrument is the ultimate resource for financial transactions, especially for small-value purchases. The recent report of the Federal Reserve on payment habits and transactions of the United States population shows that 26% of all transactions, and 40% of payments from $10 to $25 in 2019 were in cash (Federal Reserve 2020). In spite of lawmakers' support in utilizing non-cash transactions, cash in circulation (CIC) has a consistent growth (from 4% to 7% per year) in the recent five years. Statistics accentuate that CIC remains high in developed countries. For example, in Singapore which stands as a mature and developed market in electronic payment mechanisms, CIC is still high and six of ten transactions are performed by cash (Capgemini 2019). Referring to Xu et al. (2019), the rate of the CIC in the United States has increased by 82.1% between 2007 and 2016. In other countries including China, the amount of cash swirling is still high. In the past decade, these countries are faced by CIC growth rate of nearly 124% (Xu et al. 2019). Meanwhile, CIC grows drastically in countries undergoing severe distress such as Ukraine, Myanmar, and Mozambique (Capgemini 2019). The consistent growth of CIC across countries led the related organizations to put their efforts on managing the banknote supply chains in an effective way. CIT routing problem is generally studied as one of the application areas in the VRPs for transportation of valuable goods including cash and jewelry in populated cities and metropolitan areas.

In spite of employing better-armored vehicles and technological development (e.g., weapons on board, vehicle tracking), providing safe and protected transportation is still a challenging operation for CIT companies. Security considerations in route planning of CIT are pivotal in preserving the operation from heists and robberies (Smith et al. 2010, Yan et al. 2012). However, security analysis for minimizing the risks and threats may require a high-level planning and generally affect the operating costs considerably. Thereby, the safe and efficient routing scheme should be executed for the success of CIT operations. To this end, minimizing travel costs along with minimizing risks and threats should be considered simultaneously (Talarico et al. 2017a).

Traffic congestion is a major issue for both commuters and logistics companies in urban environments. This growing phenomenon considerably affects travel speeds during the rush hours. To capture the impact of traffic congestion, the time-dependent VRP (TDVRP) is introduced in the literature. This problem considers the presence of traffic patterns during the day. In this approach, time-varying speed pattern is predicted to determine an average traveling speed from one period to another. To the best of our knowledge, none of the previous works on CIT problems studied time-dependency of travel times. However, due to the importance of time factor in CIT, ignoring the traffic congestion may bring imprecise planning decisions.

Another deficiency of traditional VRPs is that many researchers consider only one edge between each pair of nodes by a simple graph network representation. By this, many feasible solutions may be discarded from the solution space. Due to the complexity of urban network, it is more plausible to reach one node from another one by multiple parallel links. These links are usually differentiated by multiple inherent attributes (e.g., travel time, distance, and risk). According to Garaix et al. (2010) and Ticha et al. (2017), simple graph network is not capable of handling routing problems when several attributes are considered on the links. To handle this, multigraph network is suggested to maintain all non-dominated available links among each pair of nodes in the network (Garaix et al. 2010). In addition, in a time-dependent environment, choosing a suited arc among the nodes of a multigraph, not only depends on traveling distance but also on the actual departure time at the origin (Setak et al. 2015). In the CIT problem, the presence of alternative links among the key-locations is extremely important and helps accelerating the operations and accessing better solutions.

Considering the multigraph network, this research aims to investigate a time-dependent CIT routing problem, which is abbreviated as a TD-CITRM. This is the first study that incorporates the effect of congestion for the CIT problems. Ignoring the speed variations not only affects logistics costs but also increases the exposure in transportation of valuable goods to a robbery in congested arteries and streets. The proposed problem is studied under both deterministic and stochastic travel speeds. In what follows, the deterministic version of the problem is called TD-CITRM-DT and the stochastic one is called TD-CITRM-ST. Due to the time-dependency, stochasticity, nonlinearity, and multigraph structure, it is computationally challenging to solve the TD-CITRM-DT and TD-CITRM-ST. To do this, we focus on proposing effective strategies to cope with the uncertainty of traffic congestion for a non-linear version of TDVRP. Finally, a real case study on cash transportation of an organization in Isfahan metropolis in Iran is provided to assess the applicability of the presented models and associated solution algorithms.

The content of this paper is structured as follows. Section 2 is dedicated to the relevant literature. Section 3 provides the problem description and preliminaries on the TD-CITRM. We formulate both deterministic and stochastic versions of the problem in Section 4. In Section 5, the procedures of the proposed algorithms are described in detail. Section 6 includes the results of various computational experiments for the models on a transportation case in Isfahan and generated instances. This section provides a sensitivity analysis on some parameters of the model and presents managerial insights and effective guidance for decision makers. Finally, in Section 7, conclusions and future research perspectives are listed.

2. Literature review

We now present the literature review in three subsections. Section 2.1 provides a brief review of time-dependent VRP studies. In Section 2.2, we overview the works that evoke multigraph representation in VRPs. A

subsequent subsection 2.3 reviewed the studies that focused on the route planning for CIT operations. Finally, we elaborate that how the current study contributes to the literature.

2.1 Time-dependent routing models

In the field of VRPs, time-dependent models have attracted a little attention. In majority of studies, the travel speed or travel time between various locations are assumed to be a constant during a day. At first, travel time variability is incorporated into VRP by Malandraki (1989) and Malandraki and Daskin (1992). They formulated the problem by a mixed-integer linear program (MILP) and applied the nearest neighbor algorithm to solve the investigated problem. Park (2000) presented a bi-criteria vehicle-scheduling problem in which the travel speeds are varied according to passing area and the time of day. One of the major weaknesses of TDVRP studies is that many of these studies do not consider the FIFO property satisfaction. Ichoua et al. (2003) involved this intuitive property in a time-dependent routing problem. In another work, Donati et al. (2003) employed the Ant Colony system to solve the TDVRP efficiently. Later, Haghani and Jung (2005) studied pick-up or delivery VRP with time-dependent travel times and soft Time Windows (TWs). The authors employed a Genetic Algorithm (GA) to solve the problem in relatively short computing times.

In another study, Figliozzi (2012) proposed an efficient solution algorithm to tackle the TDVRP with hard and soft TWs. Later, Taş et al. (2014) investigated stochastic travel times in the TDVRP where the demand nodes have soft TWs. The authors provided two metaheuristics including Tabu search (TS) and Adaptive Large Neighborhood Search (ALNS) algorithms to solve the problem. TDVRP with simultaneous pickup and delivery is studied by Zhang et al. (2014) and the authors have presented a hybrid optimization algorithm based on ant colony and TS algorithms. Wen and Eglese (2015) studied a VRP in a time-varying road network, which aimed at minimizing costs including traveling costs and congestion charge for different zones.

Other related studies in the literature focused on pollution-routing in the TDVRP, for example Jabali et al. (2012), Qian and Eglese (2016), Alinaghian and Naderipour (2016), Xiao and Konak (2016), Ehmke et al. (2016), Çimen and Soysal (2017) and Franceschetti et al. (2017). For a detailed review about time-dependent routing models, we refer to the work of Gendreau et al. (2015).

2.2 Multigraph representation in VRPs

The main advantage of studying the transportation network as a multigraph is that such network maintains alternative non-dominated links between each pair of nodes. Some of the related studies employed multigraph network to hold multiple attributes on the arcs based on Garaix et al. (2010), while other publications studied the TDVRP in a multigraph structure proposed by Setak et al. (2015). In the TDVRP according to the time that a vehicle reaches a node, passing to subsequent node by the shortest path may require more time due to the high traffic congestion, while alternative longer path may need less traveling time.

Garaix et al. (2010) incorporated alternative paths into VRP and showed that when the arcs in the underlying road network have several attributes, simple graph representation is unable to handle the problem and many available solutions may be discarded. The authors labeled the arcs of the network with two attributes time and cost (distance). Later, Lai et al. (2016) expanded the mentioned model for the heterogeneous VRP under restricted route duration limits. The authors developed TS method to tackle the additional complexity induced by the parallel arcs. In another study, Reinhardt et al. (2015) considered VRP with TWs in which a fixed charge should be paid for accessing a set of arcs. The authors analyzed their problem in both simple and multigraph network. Ticha et al. (2017) investigated the VRP with multiple-attribute parallel arcs and incorporated the TW constraint into the problem. The authors implemented a branch-and-price algorithm. In a related work, Ticha et al. (2019) provided ALNS algorithm for solving larger instances defined in Ticha et al. (2017).

The TDVRP with FIFO property is studied by Setak et al. (2015). The proposed model not only determines the sequence of demand nodes for each vehicle but also selects the proper links among available arcs based on traffic congestion. Alinaghian and Naderipour (2016) and Setak et al. (2017) investigated the application of the TDVRP in

a multi-alternative graph for reduction of environmental emissions in urban area. Huang et al. (2017) addressed a time-dependent VRP with path flexibility. The authors modeled the problem under deterministic and stochastic traffic conditions. Behnke and Kirschstein (2017) examined the impact of path selection in the emissions-minimizing. Later, Androutsopoulos et al. (2017) proposed a bi-criteria model for pollution-routing problem, which simultaneously addresses routing and path finding decisions. Similarly, Ehmke et al. (2018) developed a model for minimizing total VRP costs in a multigraph road network. The model concerns optimization of fuel consumption/emissions, distance, and time-dependent travel time. Tikani and Setak (2019) studied a reliable distribution problem in urban environments. The authors considered multi-attribute parallel links in transportation networks in disaster response operations. Their investigations showed that multigraph yields a faster and more reliable distribution process.

2.3 Cash-in-transit routing models

There are numerous studies, which deal with the VRP in different real-life applications; nonetheless, the concept of "security" in transport operations has attracted little attention in spite of its importance. Krarup (1995) and Ngueveu et al. (2010) addressed the transportation security by the context of "peripatetic" routing models. In detail, the authors forbade employing repetitive road segments where the demand nodes could be served several times. Calvo and Cordone (2003) presented an approach to reduce the risk of robberies by constructing unpredictable routes. They enforced a time lag between two successive visits for security issues. Yan et al. (2012) proposed a cash transportation vehicle routing and scheduling problem as an integer multiple-commodity network flow problem. The model strives to reduce invariant vehicle routes and schedules to increase security.

In another study, Talarico et al. (2015) formulated the CIT routing problem with a pre-specified risk threshold. Talarico et al. (2017a) developed a multi-objective mathematical formulation for CIT sector that simultaneously increases the security and minimizes the total travel cost of vehicle routes. They proposed an efficient metaheuristic to tackle the problem. Talarico et al. (2017b) provided a new metaheuristic to cope with the model introduced by Talarico et al. (2015). Moreover, Bozkaya et al. (2017) studied a bi-objective CIT routing model including transportation cost and security risk. Radojičić et al. (2018a) proposed a greedy metaheuristic with path relinking and fuzzy modification and randomized adaptive search procedure with path relinking. Xu et al. (2019) considered different cash denominations in CIT routing problem and provided a hybrid TS algorithm to solve the proposed problem.

Some of the related works studied the security of cash transportation considering TWs for each customer. For example, Talarico et al. (2013) proposed a VRP model for the CIT industry with hard TWs. Radojičić et al. (2018b) extended the TWs with fuzzy logic approach in cash distribution problem. Ghannadpour and Zandiyeh (2020) proposed a distance and risk minimization VRP model in which demand nodes impose hard TW constraints. Furthermore, four works in the literature applied time spread constraints (as a modification of TW) in cash transport operations which diversify the arrival at each customer over multiple periods. In this regard, we refer interested readers to Michallet et al. (2014), Hoogeboom and Dullaert (2019), Tikani et al. (2020a), and Soriano et al. (2020) for more details.

Since distribution of valuable goods cannot be limited to one period. Some of the presented models in the literature aim to optimize routing plans in a periodic setting. Such models include features to vary the designated routes and control the risk by preventing the reuse of already traversed links. Herein, we can refer to Yan et al. (2012), Bozkaya et al. (2017), Tikani et al. (2020a), Ghannadpour and Zandiyeh (2020) for such studies. Table 1 summarizes the studies of CIT routing problems and compares the current study to the most related works in the literature.

Table1. Summary of studies in cash-in-transit VRPs

Reference	Year	Network	Objective function		Vehicle		Risk index	Safety constraint	Route duration constraint	Traffic congestion	Uncertainty	Real transportation case	Solution algorithm			
			Objective(s)	Item(s)	Multi vehicle	Capacity							EX	HU	MH	Description
Yan et al. (2012)	2012	SGN	SO	TC	✓	×	×	×	×	×	×	✓	×	✓	×	A decomposition/collapsing method
Talarico et al. (2013)	2013	SGN	SO	TC	✓	×	✓	✓	×	×	×	×	×	×	✓	Metaheuristic algorithms
Michallet et al. (2014)	2014	SGN	SO	TC	✓	✓	×	×	×	×	×	×	×	×	✓	Local search iterative method
Talarico et al. (2015)	2015	SGN	SO	TC	✓	×	✓	✓	×	×	×	×	×	×	✓	Metaheuristics
Talarico et al. (2017a)	2017	SGN	MO	TC, R	✓	✓	✓	×	×	×	×	×	×	×	✓	A multi-objective metaheuristic
Bozkaya et al. (2017)	2017	SGN	MO	TC, R	✓	✓	✓	✓	×	×	×	✓	×	×	✓	Modified adaptive randomized bi-objective method
Talarico et al. (2017b)	2017	SGN	SO	TC	✓	×	✓	✓	×	×	×	×	×	×	✓	A hybrid meta-heuristic
Radojičić et al. (2018a)	2018	SGN	SO	TC	✓	×	✓	✓	×	×	×	×	×	×	✓	A fuzzy meta-heuristic
Radojičić et al. (2018b)	2018	SGN	SO	TC	✓	×	✓	✓	×	×	×	×	✓	×	×	The commercial solver CPLEX
Hoogeboom and Dullaert (2019)	2019	SGN	SO	TC	✓	✓	×	×	✓	×	×	✓	×	×	✓	An iterated heuristic
Xu et al. (2019)	2019	SGN	SO	TC	✓	✓	✓	✓	×	×	×	×	×	×	✓	Combined hybrid TS
Soriano et al. (2020)	2020	MGN	SO	TC	✓	✓	×	×	×	×	×	×	×	×	✓	A modified ALNS
Tikani et al. (2020a)	2020	MGN	MO	CT, R, CS	✓	✓	✓	×	✓	✓	×	×	×	×	✓	An improved NSGA-II
Ghannadpour and Zandiyeh (2020)	2020	SGN	MO	TC, R	✓	✓	✓	×	×	×	×	✓	×	×	✓	A hybrid GA
This paper		MGN	SO	CT	✓	✓	✓	✓	✓	✓	✓	✓	✓	✓	✓	Two-phase dynamic programming (DP), Two phase flexible restricted DP, Hybrid meta-heuristic using self-adaptive caching GA

Network: SGN (simple graph network), MGN (multigraph network); Objective (s): SO (Single objective), MO (Multi-objective); Item(s): TC (Transportation Cost/ Path Lengths), R (Risk), CT (Completion Time), CS (Customer Satisfaction); Solution algorithm: EX (Exact algorithm), HU (Heuristic algorithm), MH (Meta-heuristic algorithm).

In summary, we have observed that most of the proposed models in CIT routing problems are not able to reflect the real-life concerns properly. For example, CIT providers usually operate in urban regions but none of the models captures traffic congestion. The traffic condition is time-dependent and has stochastic nature on each individual link. Furthermore, researchers mainly studied the CIT in simple graph networks with multi-attribute arcs including cost (distance) and risk. However, according to the Garaix et al. (2010), simple graph networks cannot handle the problem when multiple attributes are defined on the links. These defects have motivated us to study the benefits of path flexibility for the CIT problem in multigraph networks in both deterministic and stochastic traffic conditions. More specifically, the vehicles' speeds are considered as stochastic parameters based on the two-stage stochastic programming and the scenario generation method. Hereupon, a new risk measuring approach is proposed to capture the innovative characteristics of TD-CITRMs. It is defined as a cumulative measure along each constructed route and addresses three important vulnerability factors in the risk assessment of cash distribution including time-dependent traffic congestion, existence of multi-attribute parallel links in inner-city areas and characteristics of the links. In addition, we involve maximum allowable time duration together with a risk threshold in the models to design a more balanced routing scheme. This feature helps to improve the quality of achieved solutions from the perspective of both CIT companies and financial organizations.

3. Preliminaries and problem description

The problem described in this paper deals with the transportation of valuable goods (e.g., money) in urban environments. The proposed VRP models determine the best sequence of nodes and the best link between each pair of nodes (according to the time of a day). An example for showing the necessity of considering alternative links in a CIT routing problem is provided in Figure 1. In this example, there are three options to traverse the distance between two specific nodes. The travel time and related traveling risk are illustrated. According to this figure, at 8 AM, the shortest link is 4.6 kilometers with 11 minutes' travel time, while another longer path with 5.1 kilometers is less risky and requires 10 minutes' travel time. On the other hand, in the low-traffic condition the optimum link is changed to the shortest link of 4.6 kilometers. Here, the link with 6.6 kilometers is dominated by two other links concerning their travel time and traveling risk.

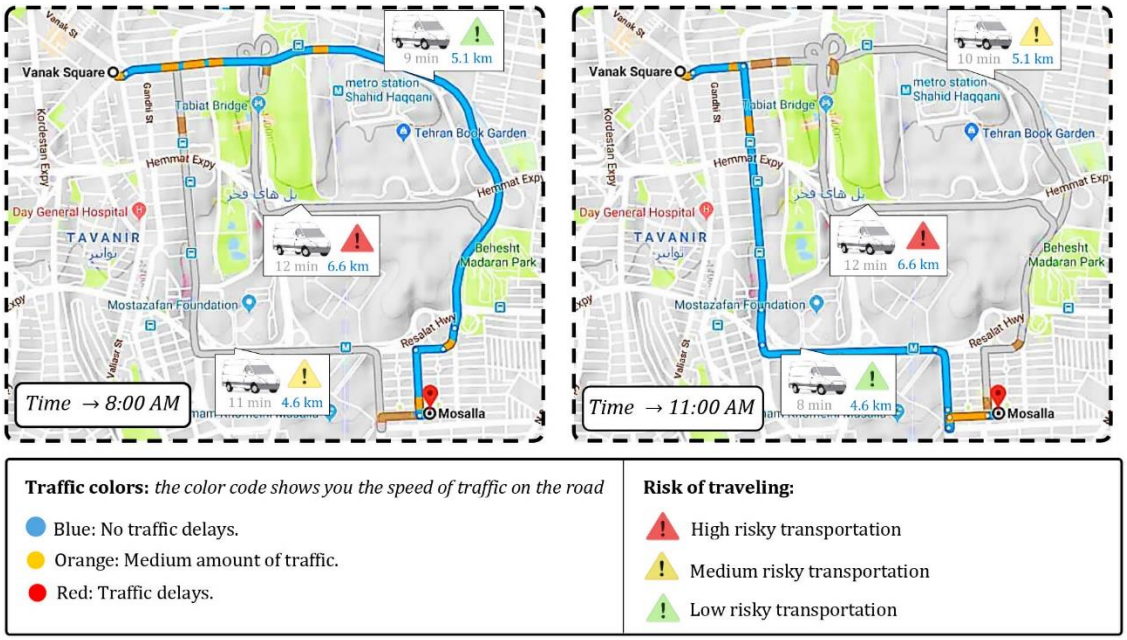

Figure 1. Available alternative links between a pair of nodes -Google maps

As mentioned earlier, the TD-CITRM-DT is modeled as a time-dependent VRP. The underlying network is considered as an oriented multigraph structure $G = (V, A)$. Vertex set V contains a central depot and a set of demand points $N = \{1, \ldots, n\}$. In addition, $A = \{(i, j, m): i, j \in V, i \neq j\}$ shows the set of traffic connections among the nodes. Each arc is represented by (i, j, m), in which m indicates the mth parallel link from nodes i to j. For the convenience of the reader, notations used in the paper are gathered in Table A.1 of Appendix A.

3.1 The consideration of FIFO property

The FIFO or the non-passing property ensures that, if vehicle A begins to travel the arc (i, j) earlier than vehicle B, then it reaches to its destination j before vehicle B. Earlier works on TDVRP did not satisfy FIFO property (Ichoua et al. 2003). In fact, they utilized a discrete function of time to model the travel times. An example of their approach is depicted in Figure 2(a). As shown in the figure if a vehicle departs the origin at 1:00, it will reach to its destination in 120 kilometers away at 4:00. Nonetheless, if a vehicle departs at 2:00, it will arrive at its destination at 3:43. This situation does not fit properly in practice because the result does not conform to the FIFO property.

Recently, researchers employ continuous travel time functions over the time horizon. Here, we utilized the transformation procedure of Setak et al. (2015) to convert a travel speed pattern into a travel time function. The inputs of this procedure are T initial time intervals with their speeds for each link, and the outputs are h new time intervals $\bar{T}_{ijm}^{h}$ and two different coefficients a_{ijm}^{h} and b_{ijm}^{h}. Let t_0 be the departure time of a vehicle which passes the mth link from node i to node j in interval $[\bar{T}_{ijm}^{h}, \bar{T}_{ijm}^{h+1}]$. Thereby, the travel time can be obtained from $t = a_{ijm}^{h} + b_{ijm}^{h} \times t_0$. By implementing this method on the travel speeds of Figure 2(a), the corresponding travel time function is obtained as depicted in Figure 2(b).

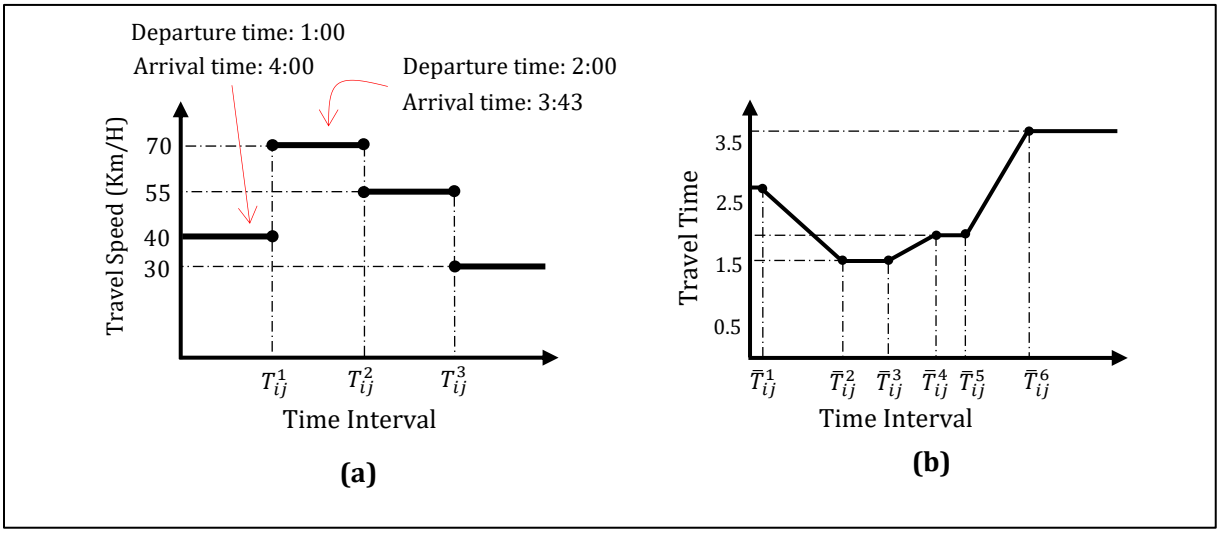

Figure 2. (a) Example of travel speed function; (b) The corresponding travel time function

3.2 Time dependency in the studied multigraph network

In traditional time-dependent routing models, the problem is constructed on a simple graph network and the travel speed change based on the congestion levels in various time intervals. However, a simple graph is only able to handle one link between each pair of nodes and discard the related parallel links. However, a multigraph representation allows us to consider alternative paths between two sequential nodes. Therefore, according to the time of the day, the link with lowest travel time among the nodes can be changed. Figure 3 illustrates the effects of time-dependent travel time on the TD-CITRM in a multigraph configuration. In Figure 3, the links with the lowest travel time are presented with continuous lines. This simple example shows that the less time-consuming arcs in multigraphs change throughout different time intervals. However, the proper link between a pair of nodes is related to both introduced attributes of arcs.

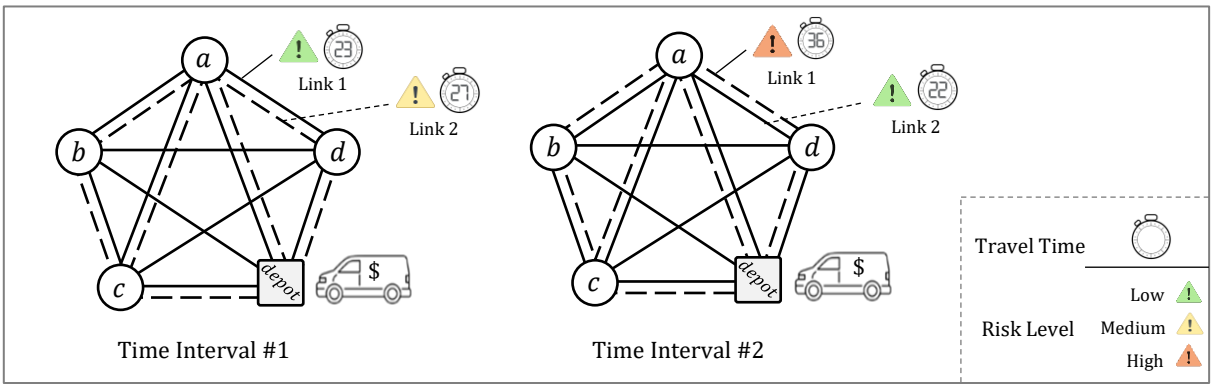

Figure 3. Time-dependent multigraph network with multi-attribute arcs (dashed lines: parallel links)

3.3 Risk measurement in multigraph

Operational risks have been thoroughly studied in the routing of hazardous materials. There are various mathematical models in hazmat transportation, which capture different risk aspects in transportation (Kumar et al. 2018; Ghaderi and Burdett 2019 and Bula et al. 2019). Generally, risk functions are defined according to the road conditions and characteristics of transported dangerous goods. In the CIT, population is not endangered and there is not any explosion probability. Instead, the vehicles are under the risk of robbery along their route. Moreover, interviews with professional experts in cash logistics indicate that cash transportation is expected to be performed in the early hours of the morning to almost before noon. Accordingly, the risk of robbery occurrence when the vehicle is stationary at the position of demand nodes during the operation time is relatively constant and has no effect on the optimal solution. Thus, this item is not incorporated in our proposed risk formula.

We define the risk of occurrence of a robbery along an edge (i, j, m) in a multigraph network by four main terms:

(a) The probability of an attack is proportionate to the travel time of a vehicle on each link. So, if the vehicle k traverses the link (i, j, m), the travel time on this link is computed by $\left(t_j^k - t_i^k - s_j\right)$, where t_i^k represents the departure time of vehicle k at node i, and s_i shows the corresponding service time.

(b) The probability of occurrence of a robbery incidence is Tr_{ij}^m which is defined per unit of time. The value Tr_{ij}^m is estimated based on several factors, such as the number of available lanes in a link, tunnels, the criminal potentials in the region, weather conditions and so on (for more information see Sakip et. al 2019, Musah et al. 2020, Davies and Johnson 2015).

(c) The probability of successful robbery after its occurrence is defined by vulnerability factor v_{ijm}. Different factors such as quality of vehicles, employed weapons, the crew skills, police delays and etc. are involved in determining the parameter v_{ijm}.

(d) The amount of losses that eventuates by the robbery. It equals to the remaining cash or valuable goods in the vehicle k after visiting node i (represented by Cp_i^k).

The risk of a successful robbery occurrence along link (i, j, m) is then represented by $r_{ijm}^k = Tr_{ij}^m . v_{ijm} . Cp_i^k . \left(t_j^k - t_i^k - s_j\right)$. For the sake of simplicity, we neglect the possibility of more than one robbery occurring along each route. Moreover, since it is difficult to estimate the vulnerability factor in real situations, a constant value is assumed for this parameter. Therefore, we omit v_{ijm}in the remainder of the paper (same as in Talarico et al. 2015). By these assumptions, the risk of route k can be described by:

$$Risk_k = \sum_{(i,j,m) \in \, route\ k} Tr_{ij}^m . \left(t_j^k - t_i^k - s_j\right) . Cp_i^k \qquad (1)$$

The variable R_j^k is then introduced to determine the cumulative risk after visiting node i along link (i, j, m) in the route k. The corresponding equation is given as follows:

$$R_j^k = Tr_{ij}^m . Cp_i^k . \left(t_j^k - t_i^k - s_j\right) + R_i^k \qquad (2)$$

In the TD-CITRM, the global risk of a route is controlled by a risk threshold ρ. Limiting the global risk helps the risk reduction efforts and assures that cash or valuable goods on the vehicles could reach the destinations by relatively safe routes. Figure 4 is provided to clarify the risk measuring process. As depicted in Figure 4 (a) a vehicle should visit three demand nodes and return to the depot. In the risk constraint VRP, both capacity constraint and risk threshold can prevent serving all demand nodes in a single tour. In particular, several solutions can be discarded, because these solutions are unable to meet the risk threshold. For instance, in Figure 4(b), the blue route cannot be used when $\rho = 5$ because the cumulative risk index at node B is $R_B^1 = \underset{0 \to A}{(0.01 \times 30 \times 4)} + \underset{A \to C}{(0.015 \times 20 \times 18)} + \underset{C \to B}{(0.001 \times 5 \times 12)} = 6.66$. An acceptable solution is shown in Figure 4(c).

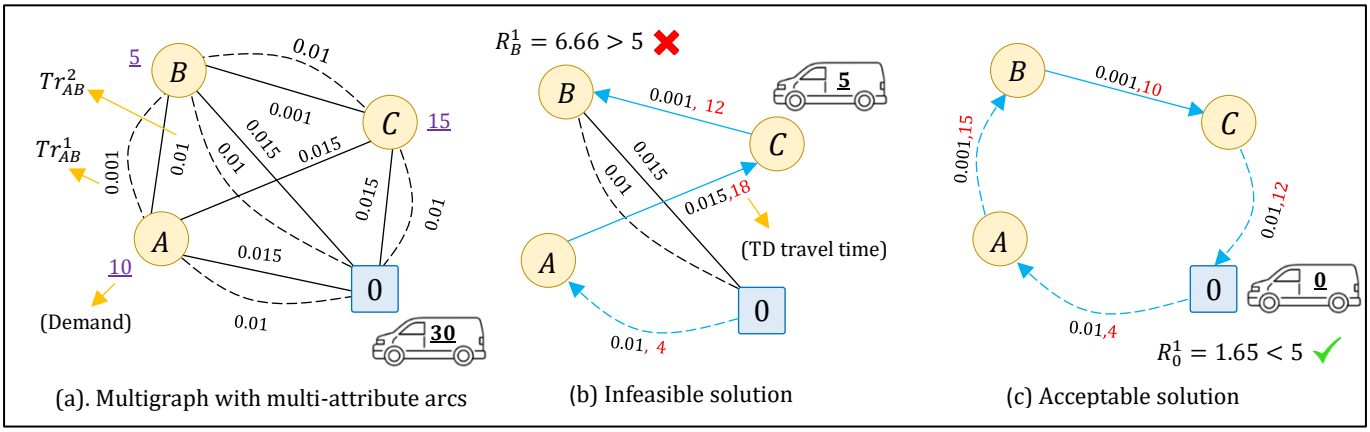

Figure 4. Risk measuring procedure for a vehicle in a multigraph network (dashed lines: parallel links)

Different criteria are utilized to increase the quality of services in VRPs. One of them is limiting route duration or route length (Cordeau et al. 2003). From a CIT company's perspective, it is more desirable that carrier operations be balanced, and the routing plans are accomplished in a certain time. In addition to the CIT companies, economic organizations as banks tend to receive their demands earlier to satisfy customers' withdrawal and increase the customer service level. In order to balance the routing plans, we consider a maximum route duration to ensure that all vehicle routes should be completed before a special time threshold.

4. Mathematical formulations

In this section, we introduce the TD-CITRM-DT as a mixed-integer non-linear programming and the related stochastic version TD-CITRM-ST using two-stage stochastic programming method. The following assumptions have been made to formulate the problem: (*i*) Vehicles are arranged to begin their carrier operations at the starting points of time intervals; (*ii*) if the expected operation time or cumulative risk on each route exceeds the given threshold values, the solution becomes infeasible; (*iii*) since the TD-CITRM is studied in urban network, it is possible to travel by using one of parallel links (multigraph representation); (*iv*) the parallel available links are characterized based on multiple attributes consisting of time-varying traffic congestions and traveling risk; (*v*) the demand associated with each location's node is known. In detail, the related organizations (e.g., banks, ATMs, and so on) should exactly specify their demands before route planning, and finally (*vi*) all of the armored vehicles have similar specifications and supposed to only deliver valuable items along their route and finally return to the depot.

4.1 Deterministic model (TD-CITRM-DT)

The TD-CITRM-DT determines both sequence of nodes and appropriate arcs between them. It aims at minimizing the sum of completion times while the cumulative risk for each route should be equal or less than a predefined risk threshold. This threshold value should be determined in a preliminary analytical stage based a series of factors such as the amount and type of valuable goods, the characteristic of road networks, and the company's attitude to risk (Talarico et al. 2015). It is worthwhile to mention that the set of candidate arcs M_{ij} includes promising arcs among each pair of nodes (i, j) and is the input parameters of the models which should be determined in advance. We now provide the decision variables below.

x_{ij}^k $\begin{cases} 1, & \text{if the vehicle } k \text{ goes from node } i \text{ to node } j \\ 0, & \text{otherwise ;} \end{cases}$

x_{ijm}^{hk} $\begin{cases} 1, & \text{if the vehicle } k \text{ moves through the } m\text{th edge from node } i \text{ to node } j \text{ in the } h\text{th time interval} \\ 0, & \text{otherwise ;} \end{cases}$

t_i^k The departure time of the vehicle k from node i;

R_i^k The cumulative risk at node i for the vehicle k ;

Cp_i^k The remaining valuable goods at node i for the vehicle k.

Using the variables and the notations of Table A.1, the proposed TD-CITRM-DT can be modeled as a mixed-integer non-linear program as follows (E is a large constant number):

Minimize $\sum_{k\in K} t_{n+1}^k$ (3)

Subject to:

$$\sum_{i\in(\{0\}\cup N),i\neq j}\sum_{k\in K} x_{ij}^k = 1 \qquad \forall j \in N \tag{4}$$

$$\sum_{j\in(\{n+1\}\cup N),j\neq i}\sum_{k\in K} x_{ij}^k = 1 \qquad \forall i \in N \tag{5}$$

$$\sum_{i\in(\{0\}\cup N)} x_{ij}^k = \sum_{i\in(n+1\cup N)} x_{ji}^k \qquad \forall j \in N, \forall k \in K \tag{6}$$

$$\sum_{i\in(\{0\}\cup N),i\neq j}\sum_{m\in M_{ij}}\sum_{h\in H_m} x_{ijm}^{hk} = \sum_{i\in(\{0\}\cup N),i\neq j} x_{ij}^k \qquad \forall j \in (N\cup\{n+1\}), \forall k \in K \tag{7}$$

$$\sum_{j\in N}\sum_{k\in K} x_{0j}^k \leq |K| \tag{8}$$

$$t_j^k - t_i^k \geq a_{ijm}^h + b_{ijm}^h t_i^k + s_j + \left(x_{ijm}^{hk} - 1\right)E \quad \forall i \in (\{0\}\cup N), \forall j \in (\{n+1\}\cup N), \forall k \in K, \forall m \in M_{ij}, \forall h \in H_m, i \neq j \tag{9}$$

$$t_i^k \geq \bar{T}_{ijm}^h + \left(1 - x_{ijm}^{hk}\right)E \quad \forall i \in (\{0\}\cup N), \forall j \in (N\cup\{n+1\}), \forall k \in K, \forall m \in M_{ij}, \forall h \in H_m, i \neq j \tag{10}$$

$$t_i^k \leq E \sum_{j\in(N\cup\{n+1\})} x_{ij}^k \qquad \forall i \in (\{0\}\cup N), \forall k \in K \tag{11}$$

$$Cp_0^k \leq Q \qquad \forall k \in K \tag{12}$$

$$Cp_0^k = \sum_{i\in N} D_i \sum_{j\in(\{n+1\}\cup N)} x_{ij}^k \qquad \forall k \in K \tag{13}$$

$$Cp_j^k \geq Cp_i^k - D_j - \left(1 - x_{ij}^k\right)E \qquad \forall i,j \in (N\cup P), \forall k \in K, i \neq j \tag{14}$$

$$R_0^k = 0 \qquad \forall k \in K \tag{15}$$

$$R_j^k \geq Tr_{ij}^m . Cp_i^k . \left(t_j^k - t_i^k - s_j\right) + R_i^k - (1 - \sum_{h\in H_m} x_{ijm}^{hk})\, E \qquad \forall i \in (\{0\}\cup N), \forall j \in (\{n+1\}\cup N), \forall k \in K, \forall m \in M_{ij}, i \neq j \tag{16}$$

$$0 \leq R_i^k \leq \rho \qquad \forall i \in (N\cup P), \forall k \in K \tag{17}$$

$$t_{n+1}^k \leq \delta \qquad \forall k \in K \tag{18}$$

$$x_{ijm}^{hk}, x_{ij}^k = \{0,1\} \qquad \forall i,j \in (N\cup P), \forall m \in M_{ij}, \forall h \in H_m, \forall k \in K \tag{19}$$

$$t_i^k, R_i^k, Cp_i^k \geq 0 \qquad \forall i \in (N\cup P), \forall k \in K. \tag{20}$$

The sum of completion times is minimized in objective function (3). Constraints (4) and (5) ensure that each node is served exactly once. Constraints (6) impose that vehicle k should leave a node if it has previously entered to that node's location. Constraints (7) enforce the vehicle to select only one link for passing node i to j. Constraint (8) assures that at most $|K|$ routes are constructed. Constraints (9) are used to determine the departure time of vehicle k at each demand node. Constraints (10) and (11) are employed for the related time interval, considering the vehicle departure time from the origin node. Constraints (12) limit the capacity of vehicles and forces that no vehicle is overloaded. Constraints (13)–(14) are employed to compute remaining cash or valuable goods from the depot to each node on the route of a vehicle. Constraints (15)–(16) propagate the risk measurement constraints. Note that constraints (16) contain nonlinear terms (the travel time is multiplied by the amount of remaining valuable goods). Constraints (17) control the cumulative risks to be equal or less than the threshold value ρ. Constraints (18) enforce that the operation time of each vehicle should not exceed the given threshold δ. Finally, constraints (19)–(20) define the variable types. We note that sub-tours are prevented using the remaining demand (Cp_j^k), the cumulative risk (R_i^k), and the departure time (t_i^k) at each node.

4.2 Stochastic formulation (TD-CITRM-ST)

To characterize the uncertainty in traffic conditions of available links, the problem is modeled as two-stage stochastic programming. In fact, a scenario tree consisting of a finite number of scenarios is employed to approximate the stochastic travel speeds in TD-CITRM-ST. To this end, we categorize the decision variables into two subsets: (*i*) scenario-independent variables (first-stage decisions) that are made prior to observing the actual realizations of the uncertain parameters. Here, decisions on the vehicle routing x_{ij}^k and the cumulative drop-offs Cp_j^k represent the first-stage actions. These variables are determined based on the expected traffic patterns using statistical analysis. (*ii*) Scenario-dependent variables (second-stage decisions) that are made after realization of all random events. Let us consider a finite set of scenarios Ω, where each $\omega \in \Omega$ is a random scenario. These variables are then likely to change for different realizations of ω and include the arc selection decisions $x_{ijm}^{hk}(\omega)$, departure time at each node $t_i^k(\omega)$, and cumulative risks for each vehicle $R_j^k(\omega)$. The two-stage stochastic non-linear mixed integer program of TD-CITRM-ST can be written as follows:

Stage one (P1):

$$\text{Minimize} \quad E_\xi\left[h\left(\mathbf{x}, \xi\right)\right] \tag{21}$$

Subject to:

$$\sum_{i\in(\{0\}\cup N), i\neq j} \sum_{k\in K} x_{ij}^k = 1 \qquad \forall j \in N \tag{22}$$

$$\sum_{j\in(\{n+1\}\cup N), i\neq j} \sum_{k\in K} x_{ij}^k = 1 \qquad \forall i \in N \tag{23}$$

$$\sum_{i\in(\{0\}\cup N)} x_{ij}^k = \sum_{i\in(\{n+1\}\cup N)} x_{ji}^k \qquad \forall j \in N, \forall k \in K \tag{24}$$

$$\sum_{j\in N} \sum_{k\in K} x_{0j}^k \leq |K| \tag{25}$$

$$Cp_0^k \leq Q \qquad \forall k \in K \tag{26}$$

$$Cp_0^k = \sum_{i\in N} D_i \sum_{j\in(\{n+1\}\cup N)} x_{ij}^k \qquad \forall k \in K \tag{27}$$

$$Cp_j^k \geq Cp_i^k - D_j - (1 - x_{ij}^k)E \qquad \forall i, j \in (N \cup P), \forall k \in K, i \neq j \tag{28}$$

$$x_{ij}^k = \{0,1\} \qquad \forall i, j \in (N \cup P), \forall k \in K \tag{29}$$

$$Cp_i^k \geq 0 \qquad \forall i \in (N \cup P), \forall k \in K \tag{30}$$

Then, for each ω, the second stage problem with the objective function $h\left(\mathbf{x}, \xi(\omega)\right)$ can be formulated as:

Stage two (P2):

$$h\left(\mathbf{x}, \xi(\omega)\right) = \text{Min} \sum_{k\in K} t_{n+1}^k(\omega) \tag{31}$$

Subject to:

$$\sum_{i\in(\{0\}\cup N),i\neq j}\sum_{m\in M_{ij}}\sum_{h\in H_m} x_{ijm}^{hk}(\omega) = \sum_{i\in(\{0\}\cup N),i\neq j} x_{ij}^{k} \qquad \forall j \in (N\cup\{n+1\}),\forall k\in K \tag{32}$$

$$t_j^k(\omega) - t_i^k(\omega) \geq a_{ijm}^h(\omega) + b_{ijm}^h(\omega)t_i^k(\omega) + s_j + \left(x_{ijm}^{hk}(\omega) - 1\right)E \quad \forall i \in (\{0\}\cup N), \forall j \in (N\cup\{n+1\}),\forall k\in K,\forall m\in M_{ij},\forall h\in H_m, i\neq j \tag{33}$$

$$t_i^k(\omega) \geq \bar{T}_{ijm}^h(\omega) + \left(1 - x_{ijm}^{hk}(\omega)\right)E \quad \forall i \in (\{0\}\cup N),\forall j\in(\{n+1\}\cup N),\forall k\in K,\forall m\in M_{ij}, \forall h\in H_m, i\neq j \tag{34}$$

$$t_i^k(\omega) \leq E\sum_{j\in(N\cup\{n+1\})} x_{ij}^k \qquad \forall i\in(\{0\}\cup N),\forall k\in K \tag{35}$$

$$R_0^k(\omega) = 0 \qquad \forall k\in K \tag{36}$$

$$R_j^k(\omega) = Tr_{ij}^m.Cp_i^k.\left(t_j^k(\omega) - t_i^k(\omega) - s_j\right) + R_i^k(\omega) - (1 - \sum_{h\in H_m} x_{ijm}^{hk}(\omega))E \quad \forall i\in(\{0\}\cup N),\forall j \in(\{n+1\}\cup N),\forall k\in K,\forall m\in M_{ij},i\neq j \tag{37}$$

$$0 \leq R_i^k(\omega) \leq \rho \qquad \forall i\in(N\cup P),\forall k\in K \tag{38}$$

$$t_{n+1}^k(\omega) \leq \delta \qquad \forall k\in K \tag{39}$$

$$x_{ijm}^{hk}(\omega) = \{0,1\} \qquad \forall i,j \in (N\cup P),\forall m\in M_{ij},\forall h\in H_m,\forall k\in K \tag{40}$$

$$t_i^k(\omega), R_i^k(\omega) \geq 0 \qquad \forall i\in(N\cup P),\forall k\in K \tag{41}$$

The constraints (21-30) in the first stage of TD-CITRM-ST are same as the deterministic formulation. While we redefined the constraints in the second stage sub-problem based on each scenario. In detail, the first stage of the model (P1) is a capacitated VRP with the objective function representing the expected value of the objective functions of second stage sub-problems (P2).

5. Solution approaches

Due to the complexity and non-linearity features of the investigated problem, exact commercial solvers cannot even handle small-sized instances in reasonable computation times. Previous related papers confirmed the high computational challenges of solving the TDVRP in a multigraph. For example, Setak et al. (2015) managed to solve a simple and linear TDVRP model in a multigraph with only six nodes in more than 7.5 hours using the CPLEX solver. While, the solution methods in the current study are capable to solve the highly constrained routing models including TD-CITRM-DT and TD-CITRM-ST in much less computation times. More specifically, the proposed two-phase DP algorithm in this study finds the exact solution for larger instances (in comparison to Setak et al. 2015) in less than five minutes. We note that the proposed solution methods in the literature are not practical for the introduced problems because the structure of our models is totally different from previous mathematical models due to the existence of time-dependent travel times, multigraph structure, and the defined attributes on the links. Thus, in what follows, three different strategies inspired from Tikani and Setak (2019) including exact, heuristic and hybrid optimization method are improved to efficiently solve the TD-CITRM-DT.

- ***Exact method:*** We develop two-phase DP based algorithm to obtain the optimal solution for the TD-CITRM-DT. To handle multiple vehicles in a single route in DP, the giant-tour representation (GTR) is applied to the VRP. The first phase of the algorithm specifies the sequencing of demand nodes. Then, in the next phase, the exact link selection procedure in a fixed sequence of nodes (LSFSN) is implemented to determine the proper links, which satisfy the risk threshold constraint.
- ***Heuristic method:*** In order to save memory usage and to prevent high computation times in previous exact algorithm, a new flexible restricted dynamic programming (FRDP) method is utilized in stage 1.
- ***Hybrid optimization method:*** To cope with larger-sized instances, a hybrid multi-phase optimization algorithm based on the genetic algorithm (GA) and DP is proposed. Then, the obtained solutions go

through LSFSN (in the second phase) to handle additional constraints. This algorithm employs caching techniques for fast exploration process and diversifies the population list using prepared internal data storage.

We modified the introduced methods in Section 5.3 to deal with the uncertainties of traffic congestions in TD-CITRM-ST. We discuss two approaches including bi-level optimization strategy and Route-Path approximation method to address this issue.

5.1 Dynamic programming method

DP method solves the problem by decomposing a complex problem into partial sub-problems (Bellman 1961). At the first phase of the proposed exact method, a forward algorithm is employed to minimize the sum of completion times over the set of vehicles by determining the sequence of nodes and their assignments to the routes. More specifically, the optimization process in the phase one prepares a sorted list of best-found solutions by only using the best links among the nodes with less traffic congestion. The cumulative risk of constructed routes is not considered in stage one. In the second phase, considering the prior objective function, the LSFSN algorithm finds the best arcs for the problem that also satisfies the risk threshold (Garaix et al. 2010). This mechanism can achieve the optimum solution because the second phase algorithm finds the best solution (according to the objective function) from the prepared sorted list that fulfills the risk threshold (See section 5.1.3).

Here, we describe a DP formulation for the time-dependent TSP which aims at finding a sequence of nodes with minimum total operation time in the generated tour. Assume that V \0 shows a set of vertexes, then a state can be defined by (Φ, j) where $j \in \Phi$ and $\Phi \subseteq$ V \{0}. In detail, the state (Φ, j) is a partial tour starting from depot 0. It also serves all demand nodes in set Φ and ends in node $\in \Phi$. Accordingly, $\bar{C}(\Phi, j)$ represents the total operation time of partial tour (Φ, j). Starting from the depot, the earliest possible arrival time at customer j in the first-time interval is $\min_m\{a_{01m}^1\}$. Therefore, the costs of the first stages $\bar{C}(\{j\}, j)$ are computed by equation (42). In accordance with the FIFO property, the costs of middle stages $\bar{C}(\Phi, j)$ are computed using equation (43). In addition, the final stages $\hat{C}$ can be computed by equation (44).

$$\textit{First}\text{ stage:}\quad \bar{C}(\{j\}, j) = \min_m\{a_{0jm}^1\} \qquad \forall j \in V \setminus \{0\} \tag{42}$$

$$\textit{Middle stages:}\quad \bar{C}(\Phi, j) = \min_{i \in \Phi \setminus j}\{\bar{C}(\Phi \setminus j, i) + \min_m\{a_{ijm}^h + b_{ijm}^h t_i^k + s_j\}\} \qquad \forall j \in \Phi \tag{43}$$

$$\textit{Final stage:}\quad \hat{C} = \min_{j \in V \setminus \{0\}}\{\bar{C}(V \setminus 0, 0) + \min_m\{a_{j0m}^h + b_{j0m}^h t_j^k\}\} \qquad \forall j \in \Phi \tag{44}$$

This method generates only one tour and is unable to directly handle VRP. To cope with this issue, a transformation should be conducted to convert a VRP solution to a feasible giant tour. Moreover, the capacity of vehicles and maximum route duration are controlled by adding extra state dimensions to the generated partial tours of DP.

5.1.1 Giant-tour representation (GTR)

GTR is a practical approach to address multiple TSP (Funke 2005). In GTR, a transformation is conducted to replace the real depot with dummy depots in the same position. Thus, for each vehicle $k = 1 \ldots |K|$, one origin node o_k and one destination node d_k is assumed. Then, to maintain all routes in a single tour, the route of vehicle k starts at node o_k and ends to d_k and the feasible expansion is o_{k+1}. It implies that the route of vehicle $k+1$ is started. To this end, the distance from o_k and d_k is assumed to be a sufficiently large number. In addition, the distance from d_k and o_{k+1} is assumed to be zero. For simplicity, instead of using start and end dummy nodes for the depot, we can merge d_k with o_{k+1} and employ one artificial separator. By this representation, we can achieve some distinct routes for the vehicles.

As mentioned before two additional state dimensions are utilized to specify the remaining capacity and remaining allowable travel time for a vehicle. By these states, we prevent the expansion of unfeasible partial tours. More specifically, an expansion for the generated partial tour Φ is acceptable only if the two conditions are satisfied: (i) there exists enough capacity for the vehicle k to satisfy all the demand nodes in the constructed partial route ($\sum_{i \in \Phi} D_i \sum_{j \in \Phi} x_{ij}^k \leq Q$), and (ii) since the algorithm employs the best links among available parallel arcs according to the travel time at the first phase, by adding node i to the route of vehicle k, the maximum route

duration should not exceed the pre-specified threshold ($t_i^k \leq \delta$ where $i \in \Phi$). It is notable that the cumulative risk of each constructed route is evaluated in the second phase using LSFSN method.

5.1.2 Flexible restricted list with weighted random sampling

Gromicho et al. (2012) implemented the restricted DP (RDP) on VRPs using GTR. The authors expanded the restricted DP of Malandraki and Dial (1996) to accelerate the operation of the algorithm. In this method, only H promising states with the lowest costs are selected to be expanded in the next stage. The reason is that low-cost states have more chance to reach a better solution compared to high-cost states.

Soysal and Çimen (2017) utilized weighted random sampling to form the restricted list in the RDP. Their algorithm selects $H + S$ partial tours to be expanded in the next stage, where S partial tours are picked out using weighted random sampling. Moreover, Tikani and Setak (2019) introduced RDP with a dynamic restricted list. The authors expressed that applying restrictions in the initial stages of RDP yields to lose feasible solutions. Because most of the nodes are not considered in the states of initial stages. Conversely, by tending to the final stage, most of the nodes are added to the states and lower ranks states have less chance to achieve proper solutions. In this study, we integrate these two efficient strategies with some modifications and present a new heuristic method based on DP with flexible restriction list and weighted random sampling. At each stage of FRDP, the algorithm follows the procedure stated in Algorithm 1. The n in Algorithm 1 shows the stage number.

Algorithm 1. The steps of the proposed FRDP

Step #1	Define potential partial tours for the current state, based on the available states from the previous stage and non-attended demand nodes.
Step #2	Calculate the time dependent operation cost $\bar{C}(\Phi, j)$ for each constructed partial tour using equation (43). For the initial stage use equation (42).
Step #3	Rank all generated states based on their costs in ascending form.
Step #4	Calculate the size of restricted list → $\text{SRL}_n = [1.5 \times \bar{H}] - \left[\frac{n}{NO} \times \bar{H}\right]$, where NO represents the total number of stages and $\bar{H}$ shows approximated average width among all stages ($\bar{H}$ is defined by the decision maker).
Step #5	Compute the weights of next SRL_n remaining (not selected) states (put them in set φ). For each partial tour Φ, the corresponding weight can be achieved by: $$W(\Phi, j) = \frac{\sum_{(\Phi', j') \in \varphi} \bar{C}(\Phi', j') - \bar{C}(\Phi, j)}{\sum_{(\Phi', j') \in \varphi} \bar{C}(\Phi', j') \times (\text{SRL}_n)}$$
Step #6	Assign the cumulative probabilities of each state in set φ. For this purpose, sort the states according to their weights in ascending form $\{ W(\Phi, j)_1, W(\Phi, j)_2, \dots W(\Phi, j)_{\text{SRL}_n}\}$. Then determine the cumulative weights (CW) as follows: $$CW(\Phi, j)_1 = W_1(\Phi, j)$$ $$CW(\Phi, j)_i = CW(\Phi, j)_i + (\Phi, j)_i \quad i \in \varphi \backslash \{1\}$$
Step #7	Select $2(NO - n)$ states for expanding in the next stage using weighted random sampling.
Step #8	Merge the list of SRL_n with $2(NO - n)$ selected partial tours to be expanded in the next stage.
Step #9	If all nodes are attended to the GTR, calculate the total travel cost by equation (44), otherwise return to Step #1.

5.1.3 Link selection procedure

The proposed DP (or FRDP) handles the TD-CITRM without the risk constraint and presents a set of best-found solutions $\Lambda = \{S_1, S_2 \dots, S_U\}$, which are sorted in ascending form in terms of objective value. The set Λ is the input of the second phase LSFSN optimization method that focuses on link selection procedure. The LSFSN investigates the risk threshold for the mentioned set by starting from the lowest-cost solution. Herein, Algorithm 2 is presented to get the lowest-cost sequence among Λ that fulfills the risk threshold.

In Algorithm 2, it is obvious that S_1 is the optimal solution if it satisfies the risk threshold, because S_1 has the lowest-cost objective function. Otherwise, for $(i > 1)$, S_i is not necessarily the optimum solution. Because there may exist a better solution in $\Lambda' = \{S_1, S_2 \dots, S_{i-1}\} \subset \Lambda$ which satisfies the risk threshold and has a lower cost by

employing alternative links. Therefore, we should compare the S_i with the feasible solutions that can be generated by changing the parallel links in Λ'. To handle this point, LSFSN is devised to select proper arcs in a fix sequence of nodes. More precisely, we aim to solve a sub-problem of TD-CITRM-DT, which should be solved for each route separately. Let us demonstrate each vehicle route by an acyclic directed multigraph $G_{FS} = (V_{FS}, E_{FS})$, where $V_{FS} = \{0, v_1, \dots, v_q\}$. In G_{FS}, each node has one specified predecessor and one specified successor.

Algorithm 2. Finding the lowest-cost sequence that fulfills the risk threshold

```
Input data: Set Λ = {S_1, S_2 ..., S_U}, risk threshold (ρ)
Initialization: i ← 1
While (risk threshold is not satisfied) do
    If (i ≤ U) then
        If (the sequence S_i satisfy the risk threshold) then
            If i = 1 then
                S_1 is the optimal solution of the problem
                Break;                          //End the algorithm since an optimal solution is found
            Else
                S_i is the lowest-cost sequence among Λ that fulfills the risk threshold
                Break;                          //End the algorithm
            End If
        End If
    Else
        No feasible solution is found among Λ    //Infeasible solution
    End If
    i ← i + 1
End While
Return (i, S_i)
```

Additional decision variables used in the model is listed below.

y_{im}^h $\begin{cases} 1, & \text{if the } m\text{th link from node } i \text{ to its corresponding successor node is selected in the } h\text{th time interval} \\ 0, & \text{o.w.;} \end{cases}$

t_i Departure time of the vehicle at node i;

R_i The cumulative risk at node i ;

Cp_i The remaining valuable goods at node i.

Using the notations and variables in Table A.1, the mathematical formulation of LSFSN for one route is given as:

$$\text{Minimize} \quad t_{n+1} \tag{45}$$

Subject to:

$$\sum_{m \in M_{v_i v_{i+1}}} \sum_{h \in H_{m_{v_i v_{i+1}}}} y_{v_i m}^h = 1 \qquad \forall v_i \in V_{FS} \tag{46}$$

$$t_{v_{i+1}} - t_{v_i} \geq a_{v_i v_{i+1} m}^h + b_{v_i v_i+1 m}^h t_{v_i} + s_{v_i+1} + \left(y_{v_i m}^h - 1\right) E_1 \quad \forall v_i \in V_{FS}, \forall m \in M_{v_i v_{i+1}}, \forall h \in H_{m_{v_i v_i+1}} \tag{47}$$

$$t_{v_i} \geq \overline{T}_{v_i v_{i+1} m}^h + \left(1 - y_{v_i m}^h\right) E \qquad \forall v_i \in V_{FS}, \forall m \in M_{v_i v_{i+1}}, \forall h \in H_{m_{v_i v_{i+1}}} \tag{48}$$

$$t_{v_i} \leq E \sum_{m \in M_{v_i v_{i+1}}} \sum_{h \in H_{m_{v_i v_{i+1}}}} y_{v_i m}^h \qquad \forall v_i \in V_{FS} \tag{49}$$

$$Cp_{v_{i+1}} = Cp_{v_i} - D_{v_i} \qquad \forall v_i \in V_{FS} \tag{50}$$

$$R_{v_{i+1}} \geq Tr_{v_i v_{i+1}}^m . Cp_{v_i}^k . \left(t_{v_{i+1}} - t_{v_i} - s_{v_{i+1}}\right) + R_{v_i} - \left(1 - \sum_{h \in H_{m_{v_i v_{i+1}}}} y_{v_i m}^h\right) E \quad \forall v_i \in V_{FS}, \forall m \in M_{v_i v_{i+1}} \tag{51}$$

$$0 \le R_{v_i} \le \rho \qquad \forall\, v_i \in V_{FS} \tag{52}$$

$$t_{n+1} \le \delta \tag{53}$$

$$y_{v_i m}^{h} = \{0,1\} \qquad \forall\, v_i \in V_{FS}, \forall m \in M_{ij}, \forall h \in H_{m_{v_i v_{i+1}}} \tag{54}$$

$$R_{v_i} \ge 0 \qquad \forall\, v_i \in V_{FS}. \tag{55}$$

The objective function (45) minimizes the operation time of one specific route. Constraints (46) ensure that only one link is selected to pass from node v_i to its successor node in one-time interval. Constraints (47) express the departure time at each node v_{i+1} based on its predecessor v_i. Constraints (48-49) determine the related time interval using departure times. Constraints (50) compute remaining load from the depot to each node on the route. Constraints (51) calculate the cumulative risk at each node. Constraints (52) impose the threshold value for the cumulative risk at each demand node. Constraints (53) control the duration time. Constraints (54-55) define the types of decision variables.

The LSFSN method extends a set of non-dominated labels. Both feasibility checking and utilizing dominance rules decrease the cardinality at each stage. The dominance rules that discard non-promising labels in the searching process are described here. The expansion l^1dominates l^2 (both partial routes terminate at same node q) only if the two following conditions are satisfied: (i) $t_{l^1} \le t_{l^2} \rightarrow$ It means that visiting all nodes in l^1 takes less time than l^2 (it is less time-consuming) and (ii) $R_{l^1} \le R_{l^2} \rightarrow$ It means that cumulative risk at node q in l^1 is less than l^2.

The procedure of LSFSN labeling algorithm is summarized in Algorithm 3. In this method the main loop is repeated for $|V_{FS}|$ iterations and in each iteration q, a set of labels L_q (non-dominated) represent the available paths from the depot to v_q.

Algorithm 3. LSFSN labeling algorithm

Input data: directed multigraph $G_{FS} = (V_{FS}, E_{FS})$, input parameters of the model
Initialization $p \leftarrow |V_{FS}| - 1, t_0 \leftarrow 0, R_0 \leftarrow 0, Cp_i \leftarrow \sum_{i \in V_{FS}} D_i$
For: $q \leftarrow 0$ *to* p **do**
  For each: link $m \in M_{v_q v_{q+1}}$ from v_q to its successor **do**
    Find the corresponding time interval h based on t_{v_q} (using $\bar{T}_{ijm}^{h}$)
    l: the extension of passing node v_q to its successor by arc $m \in M_{v_q v_{q+1}}$
    Calculate the information of extension l including $\{t_{v_{q+1}}, R_{v_{q+1}}, Cp_{v_{q+1}}\}$
    If (extension l is infeasible**) then**
      break; *// The maximum time duration or risk threshold is violated*
    Else
    Dominated ← false;
      For each $l' \in L_{v_{q+1}}$ **do**
        If ($l'$is dominated by l**) then**
          Delete l' from the set L_{q+1} ($L_{q+1} := L_{q+1} \backslash \{l'\}$)
        Else if (l is dominated by l'**)**
          Dominated ← true;
          break;
        End if
      End for
      If Dominated =false **then**
        Add l to L_{q+1}($L_{q+1} := L_{q+1} \cup l$)
      End if
  End for
End for
Return the lowest-cost label in L_p

5.2 Hybrid optimization method using caching GA and LSFSN

In this section, a new extension of GA named self-adaptive caching GA (SCGA) is devised to obtain near-optimal solutions for the problem. This method is hybridized by the exact LSFSN method and operates in two stages and is named as HSCGA. In the first stage, the metaheuristic part (SCGA) optimizes the TD-CITRM-DT without considering the risk threshold and determines the sequence of nodes using less time-consuming arcs. The SCGA benefits a self-adaption operation to employ various genetic operators according to their scores, simultaneously.

In the second stage, a limited number of stored items ($\mathcal{B}$) in the cache table are selected to go through the second phase optimization process LSFSN. In our study, we applied a continuous representation structure for the chromosomes because it provides smoother search. The employed crossover operators are one point, two points, and uniform. Moreover, instead of using inefficient simple mutations (e.g., swap or insertion), we embed local search (LS) strategies including well-known 2-opt, relocation of one node, and exchanging two nodes to manipulate the solutions. The algorithm chooses one of the introduced LS methods according to its probability. Then, the selected LS examines the $O(n^2)$ neighborhoods and the best solution among the initial parent and its neighbors is added to the main population. For more information about local search procedures see Prins (2009). We mention that infeasible solutions can be generated, but the resulted violations in these constraints are penalized by related positive terms.

To take advantages of several mutation and crossover strategies in GA, Zhalechian et al. (2016) introduced an approach named self-adaptation mechanism. In detail, in the pre-optimization phase, each introduced operator is scored using a specific procedure and then according to the operators' scores, selection probability metrics are assigned to the operators. In the following, in the main optimization process, the roulette wheel selection utilizes these probabilities to use one of the operators. In this regard, we employed three strategies for local searches including 2-opt, relocation of one node, exchanging two nodes and three crossover methods including one point, two point, and in the proposed SCGA.

The SCGA benefits caching strategy, which leads to improve the run-time performance and accelerate the exploration process by storing repetitive solutions during the optimization process (Tikani et al. 2020b). More precisely, once a repetitive genetic code is met, in subsequent generations, the related fitness is evoked from the provided cache memory. The existence of repetitive genetic materials on the populations may lead to a premature convergence and achieving a sub-optimum solution (Matic et al. 2017).

5.3 Uncertainty handling in the solution approaches

This section provides two solution approaches including a bi-level optimization method and Route-Path approximation method to cope with the uncertainties of TD-CITRM-ST.

Since the uncertainty in traffic congestions is represented by a set of finite scenarios, the deterministic equivalent problem (DEP) of TD-CITRM-ST can be derived out by expanding the second stage of the model using associated probabilities. The DEP version of TD-CITRM-ST is exactly equivalent to the original one, but it is much easier to be solved. Here, for solving the TD-CITRM-ST, we proposed a bi-level optimization method (Tikani et al. 2018). The basic idea is that we break up the two-stage stochastic program into two problems including route construction problem (master problem) and arc selection problems (sub-problem). After constructing each routing scheme in the master problem (or partial route in FRDP and DP), the LSFSN is reprocessed for each scenario to optimize the arc selection problems based on the sequence of nodes. Then, the expected objective value is computed with employed arcs in different scenarios. In particular, the methods are modified according to the following explanations:

DP and FRDP: In these methods, at each stage after constructing a partial tour Φ, the LSFSN method is repeated for each scenario ω using Φ. Let $\dot{C}(\Phi, j, \omega)$ be the objective function of the partial tour Φ in scenario ω and $p(\omega)$ represents scenario probability. Then, the expected objective value $\ddot{C}(\Phi, j)$ is computed by the following equation:

$$\ddot{C}(\Phi, j) = \sum_{\omega \in \Omega} p(\omega) \times \dot{C}(\Phi, j, \omega) \quad \forall j \in \Phi \tag{56}$$

In Step 2 of Algorithm 1, the equation (56) should be employed to calculate the cost of each constructed partial tour. At the final stage, the best-found solution is given according to the expected costs of constructed complete tours.

Hybrid optimization method (for HSCGA): in this method, the modified GA finds different tours for each vehicle and then to take advantage of the optimal solutions; the LSFSN exact method is re-used to obtain the optimal links on each scenario. Then, the expected objective value is calculated for each individual based on scenario probabilities.

Fitness evaluation with caching mechanism for both TD-CITRM-DT and TD-CITRM-ST is described in Algorithm 4. Moreover, the complete procedure of proposed SCGA is given in Algorithm 5.

Algorithm 4. Fitness evaluation by caching mechanism (FECM)

Input (chromosome CH, parameters of *TD-CITRM-DT* or *TD-CITRM-ST*)
Decode the CH
If (individual CH is existed in the cache table)
  If (individual CH is repetitive in the current population)
    Set the fitness value of CH to upper bound UP
  Else
    Use the cache table to achieve the fitness value of CH
  End if
Else
  Calculate the fitness value of CH using POF*
  Update the cache table based on the CH and its fitness value *// for TD-CITRM-DT*
  For each scenario
    For each route of CH
      Run LSFSN and achieve the solution that fulfills the risk threshold
    End for *// for TD-CITRM-ST*
  End for
  Calculate the fitness value of CH using EPOF*
  Update the cache table based on the CH and its fitness value
Return the achieved fitness value of CH

* POF: penalized objective function, EPOF: expected penalized objective function

Algorithm 5: Proposed hybrid self-adaptive caching genetic algorithm with local search (HSCGA)

Input Parameters: $Popsize$, P_C, P_{LC}, *coefficients* θ *and* φ
Set $UP \leftarrow \infty$, $It \leftarrow 1$
Generate an initial random population POP_{It}
For each chromosome $CH \in POP_{It}$
  If (CH is repetitive)
    Use cache table to achieve the fitness value
  Else
    Decode the CH, calculate the related fitness value and update the cache table
    Update the UP based on fitness value of CH
  End if
While (termination criteria is not satisfied) **do**
  Choose two parents from POP_{It} using *Tournament Selection*
  Apply self-adapted crossover to generate offsprings
  Evaluate the fitness values of offsprings by FECM
  Apply self-adapted local search to generate offsprings with probability P_{LS}
  Evaluate the fitness values of offsprings by FECM
  Rank the individuals of the current population and determine new population
  If (exist some individuals with fitness value UP)
    Replace these repetitive individuals with some randomly generated individuals
  End if
  $It \leftarrow It + 1$
End while
Return The best individual in the last population *// for TD-CITRM-ST*
Send The best ten individuals of the last population as sorted list $\mathcal{B}$ to the next phase
Run Algorithm 2 and find the lowest-cost sequence that fulfills the risk threshold in list $\mathcal{B} \rightarrow (i, S_i)$
For n: 1 to i *// for TD-CITRM-DT*
  Run arc selection procedure for S_n using **Algorithm 3** to satisfy the risk threshold
End for
Compare the achieved solutions and return the best solution for the problem

Solving stochastic TD-CITRM-ST by proposed bi-level optimization approach may be time-consuming in some cases. Accordingly, we modified the Route-first-Path-second approximation method (RPAM) proposed by Huang et al. (2017). In this method, first, we solve the TD-CITRM-DT with expected traffic condition. Afterward, a list of best-found solutions (provided by SCGA or FRDP) goes through arc selection procedure same as Section 5.1 to give the best-obtained solution.

6. Numerical experiments

We first provide the applicability of TD-CITRM-ST by studying a real-life transportation case. Then, the performance of the proposed models and solution algorithms are evaluated using generated instances.

6.1 Real-life transportation case

Isfahan is located in central part of Iran and is one of the most populated cities of the country. This metropolis plays a significant role in terms of tourist attractions and industrial development. In this study, we utilized the data from a real-world bank in Isfahan metropolis. In this example, the currency banknotes should be distributed from the central branch, which is located in Azadi square to automated teller machines (ATM) dispersed in the city.

The distribution operation starts at 8:00 AM and each route should be finished before 10:00 AM. Moreover, the risk threshold is $\rho = 2$. We intend to design the routing scheme for the transportation network with 20 nodes (including one depot and 19 ATMs) using two vehicles. The waiting time at each demand node is 4 minutes on average. Each employed ATM has four cash cassettes in which the capacity of each cassette is two thousand banknotes. Generally, the cassettes are filled by banknotes with values of 5,000 and 10,000 Toman (the currency of Iran). Therefore, each filled ATM contains 40-80 million Toman. Accordingly, in this case, the demand of each point is assigned within the ranges [30; 80] million Toman. Note that in real-life, the demands are known, and the related operators should determine their demands by an available electronic system in advance.

The weight of each employed banknote is 1.3 gram and the load capacity of the vehicle for both cargo and CIT personnel is approximately 6,000 kg. Thus, the maximum vehicle's capacity is set to 400K banknotes. It equals to 2-4 billion Toman. Nonetheless, due to some considerations, the maximum amount that a vehicle can carry is limited to 600 million Toman. To determine the traveling risk, we applied the statistics on the robbery occurrence to categorize the districts of Isfahan. Figure 5 illustrates the location of 15 geographically dispersed districts in Isfahan. The districts are colored based on the risk of robbery occurrence. The probability of a robbery happening on the links is estimated based on this categorization and using polls of region's experts about the road conditions.

The area is classified into three traffic zones (including light, medium, and heavy) based on their traffic patterns in Figure 6. The classification is based on the transportation statistics in Isfahan metropolis. In Figure 6, the zones with light traffic zones are distinguished by green color, those related to medium traffic are represented with pink color, and the rest which is placed in the center of the region is for heavy traffic zones.

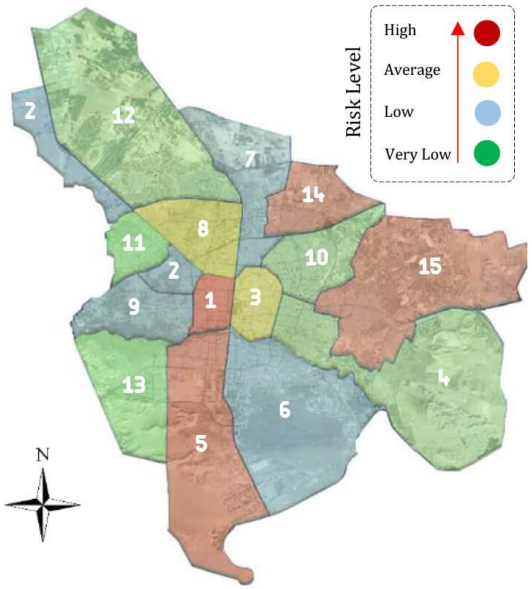

Figure 5. Districts of Isfahan and risk of robbery occurrence in each district

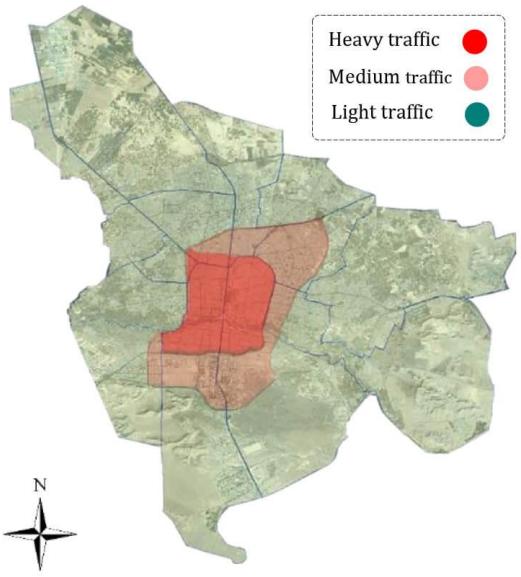

Figure 6. Traffic zones with three traffic patterns

Two scenarios $S(1), S(2)$, each with different traffic speed are explicitly taken into account. The corresponding probabilities are 60%, 40% respectively, where $S(2)$ has a higher traffic load with a less associated probability. Figure 7 shows the speed patterns for each traffic zone and for each scenario. Figure 8(a) illustrates the locations of depot and demand nodes in the underlying transportation network.

By solving the TD-CITRM-ST for the real transportation case, two routes are obtained to deliver the banknotes to all demand nodes. Figure 8 (b) represents the fleet of vehicles on each route. In this figure, if the selected link in the first and second scenario was different, the second one is depicted by dash lines. In Figure 8, $\mathcal{OBj}$ expresses the objective value. Moreover, in this figure, the completion time and cumulative risk for each route are reported.

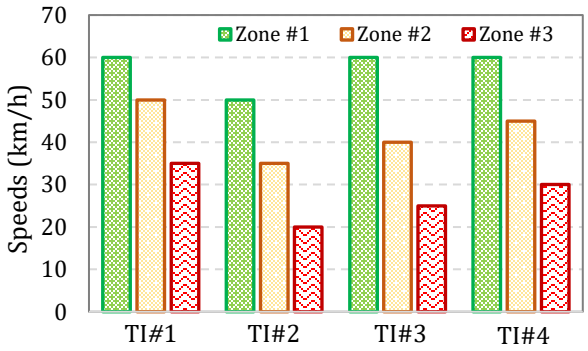

(a)Speed changes in $S(1)$

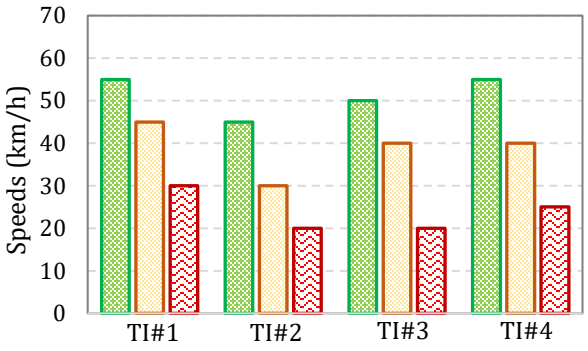

(b) Speed changes in $S(2)$

Figure 7. (a) Speed changes at different time intervals (TI) in tree zones; zone#1: heavy traffic, zone#2: medium traffic, zone#3: light traffic.

6.1.1 Results and discussion on the real case

Assume that transportation from node i to node j by link m in the first scenario and by link m' in the second scenario is represented by $i \overset{m,m'}{\longrightarrow} j$. In the studied model, the cumulative risk that each vehicle may incur in its operations is controlled by a threshold ρ'. By this, the obtained routes are route 1, $(1 \overset{1,1}{\rightarrow} 5 \overset{1,1}{\rightarrow} 7 \overset{1,1}{\rightarrow} 18 \overset{1,2}{\rightarrow} 19 \overset{1,1}{\rightarrow} 9 \overset{1,1}{\rightarrow} 11 \overset{1,1}{\rightarrow} 12 \overset{1,1}{\rightarrow} 10 \overset{1,1}{\rightarrow} 4 \overset{1,1}{\rightarrow} 2 \overset{1,1}{\rightarrow} 1)$ and route 2, $(1 \overset{1,1}{\rightarrow} 13 \overset{1,1}{\rightarrow} 15 \overset{1,1}{\rightarrow} 14 \overset{1,1}{\rightarrow} 16 \overset{1,1}{\rightarrow} 20 \overset{1,1}{\rightarrow} 17 \overset{1,2}{\rightarrow} 8 \overset{1,2}{\rightarrow} 6 \overset{1,1}{\rightarrow} 3 \overset{1,1}{\rightarrow} 1)$ with the cumulative risks of 1.5433 and 0.8051, respectively. Now we change the threshold value to $0.75\rho'$. Clearly, decreasing the risk level may eventuate a different optimum solution with higher objective value. As indicated in

Figure 8 (c), in this case, two links in the first route are replaced by their parallel link, which caused to satisfy the defined threshold value. Therefore, the two changes that occur in the resulting route is $19 \overset{1,1}{\rightarrow} 9$ and $9 \overset{1,2}{\rightarrow} 11$ that bring a slight increase in the completion time of route 1. Meanwhile, ignoring the parallel links and using simple graph network (including shortest links between each pair of nodes) lead to structural changes in the vehicle-demand node assignments (See Figure 8 (d)). In this case, the resulting routes are route 1, (1→5→7→19→9→11→12→10→4→2→1) and route 2, (1→13→15→14→16→20→17→18→8→6→3→1). The corresponding objective function is 3.3848. More specifically, we observe $\frac{(3.3848-3.2352)}{3.2352} \times 100 \simeq 4.62\%$ saving in the sum of completion times by preserving non-dominated parallel links in the solution space with multigraph representation.

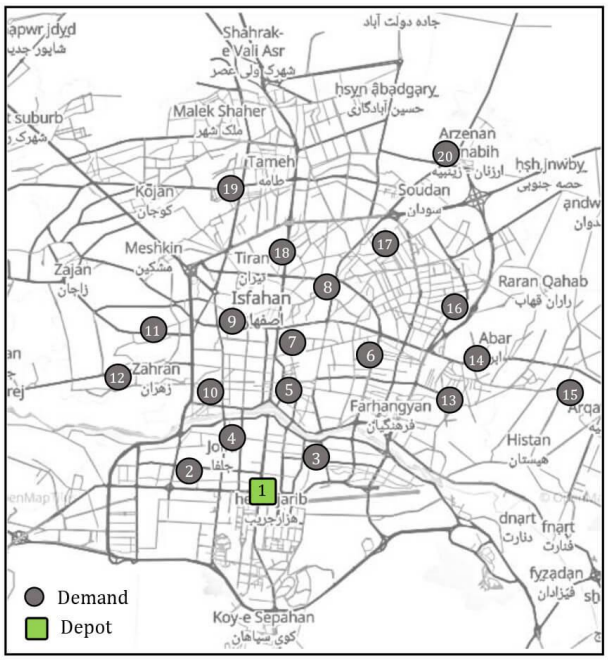

(a). Depot and demand nodes locations for the transportation case

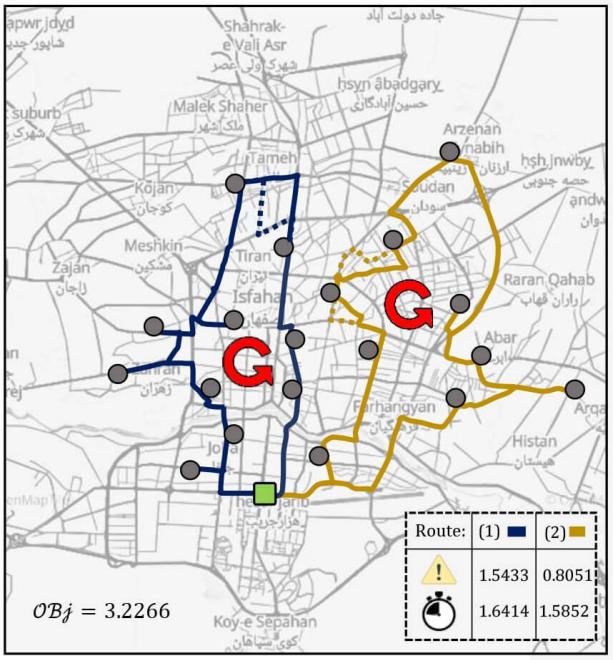

(b). Routing scheme for the transportation case in multigraph

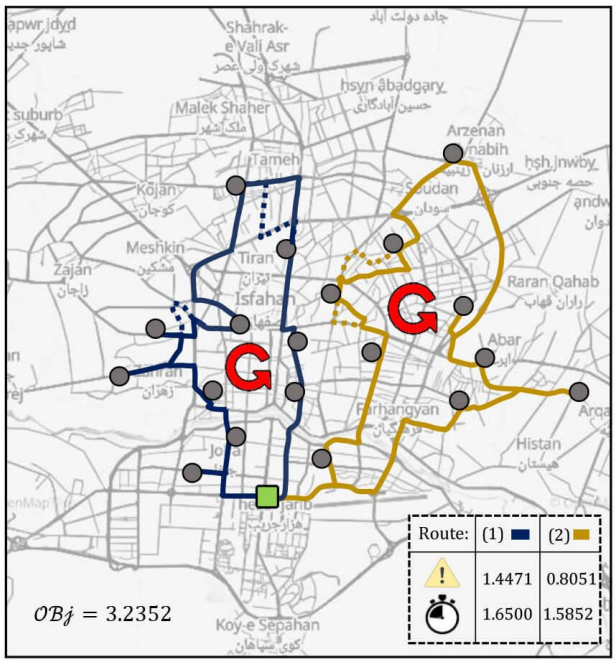

(c). Routing scheme for the transportation case with $0.75\rho'$ in multigraph

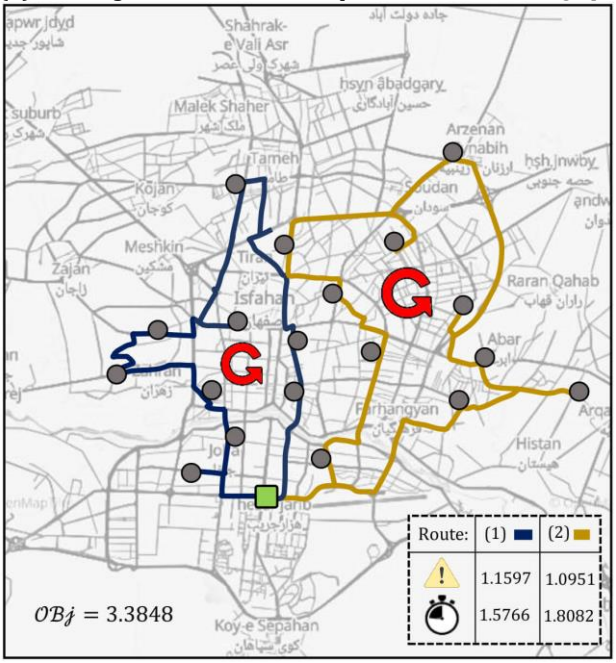

(d). Routing scheme for the transportation case with $0.75\rho'$ in simple graph

Figure 8. The locations of nodes in the transportation case and the resulting routing scheme

As discussed earlier, in the proposed models the actual travel time on each transportation link depends on starting time at its predecessor node. All previous experiments are conducted based on the assumption that the vehicles leave the depot and start their delivering operation at 8:00 AM. Here, we investigate the routing completion time and the cumulative travel risk by starting time for the 8:00 AM to 10:00 AM at fifteen minutes intervals. In order to achieve feasible solutions, δ is set to 4 hours. Figure 9 shows the objective function of the problem and travel risk of each route in different starting times. The figure indicates that if the vehicles start later than 8:00 AM, they are stuck in traffic, which increases the risk of exposure. This situation is getting worse as we close to 9:00 AM. Afterward, the traffic condition is gradually getting out of morning peak. Nevertheless, delivering the cash to demand points and finishing the operation as soon as possible is more desirable for financial organizations like banks. Because the lack of sufficient inventory of banknotes may potentially cause inconvenience to users.

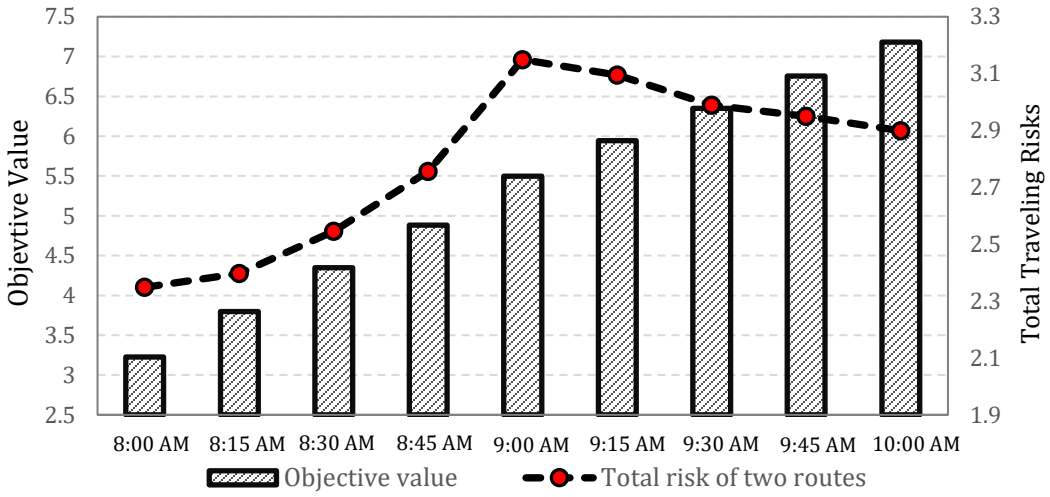

Figure 9. Analyzing the impact of starting time on the objective function and risk of traveling

Figure 10 illustrates the relation between the risk threshold ρ' and the total completion time of constructed routes in the real case study. In this case, the problem is tested by multiplying ρ' by different values. The sum of the cumulative risks for two vehicles' routes is presented by the bars, while the dashed line shows the objective function of the problem. The graph reveals the trade-off between the total travel time and transportation risk. In short, decreasing the risk threshold increases the total travel time, as expected.

It is worth mentioning that although the vulnerability factor is taken constant among the links in the case study, the probability of robbery occurrence is different for the links according to their features. Thus, by decreasing the risk threshold ρ', the model is forced to choose the best group of links that can respect the determined threshold. In this case, as expected, the objective function is increased since the model strives to handle a tighter risk constraint, which is then not achievable with employing less-time consuming arcs but instead with using the links with less probability of robbery occurrence. In addition, regarding the amount of cash carried along a route, a vehicle may spend more time on a route but with less exposure of the transported goods to robbery due to putting the customers with higher demands in an earlier position of a route. More specifically, in some cases, this prioritization may increase the completion time of a route but can meet a tighter risk limit.

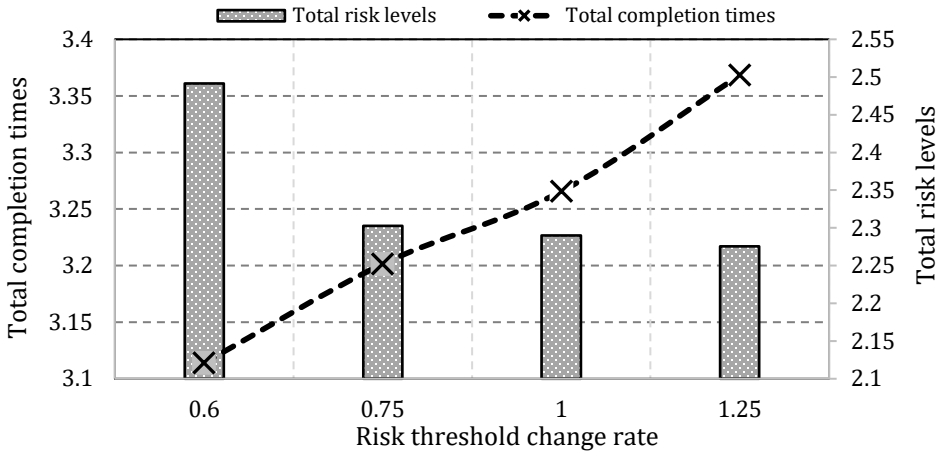

Figure 10. The relation between total risk levels and total completion times for different risk threshold

6.2 Algorithms compared

The existing datasets in the literature are not practical for the TD-CITRM-DT and TD-CITRM-ST due to several incorporated elements such as traffic congestion, multigraph network, route duration constraint etc. Therefore, we used the procedure of Appendix B to generate three sets of instances with variability in time intervals, demands, and service time for our problems. In what follows, the generated samples are named TD-CITRM_N_K where N and K denote the number of nodes (including depot) and the number of available homogeneous vehicles with capacity 500, respectively. The algorithms were implemented in MATLAB 2015a software and all experiments have been performed on a device with 6 GB RAM and an Intel core i5-3337U. 1.8GHz processor.

All the results and analysis in the main context of the paper are done by dataset 1 and detailed results for the instance of dataset 2 & 3 are provided in Appendix C. Table 2 demonstrates the obtained solutions of the DP (exact method) and FRDP heuristic. The objective functions and computation times (in second) for termination of DP are presented in Table 2 for both deterministic and stochastic variants of the problem. In this table, the TD-CITRM-ST is solved by RPAM strategy.

We implement the FRDP on the problems with five different restriction settings. Then, for each setting, the FRDP is executed ten times. The column "Best objective" shows the best-found solution among ten executions. Moreover, columns "Avg-time" and "Avg-GAP" give the average computation times and the average of gaps between the solutions returned by each run and the best-obtained solution among all proposed methods. The gap indicates the quality of solution based on the formulation $GAP = \left(\frac{\text{Found objective value} - \text{The best objective value}}{\text{The best objective value}}\right)$. If the DP method cannot find the optimum solution for an instance, the corresponding column is marked with $(-)$. Moreover, in some cases, the restriction procedure may yield the FRDP not to find any feasible solution. Thus, the column $(Acc - Sol)$ shows the number of acceptable solutions found by the algorithm among ten executions.

Referring to the results of Table 2, the FRDP with $\bar{H} = 10$ is unable to solve the examples with more than nine customers because this size of restriction is not sufficient to keep any feasible solution in the prepared list. This insufficiency also occurred in $\bar{H} = 50$ for some cases. As a rule, by increasing the restriction size of FRDP, the algorithm consumes more computation times and reaches better solutions.

Table 3 reports the results of running the examples by HSCGA and simple GA-LSFSN. In the GAs, the population size, maximum iteration, crossover percentage, and local search probability are set to 100, 200, 0.60, and 0.15, respectively. Again, the TD-CITRM-ST is solved by RPAM strategy. The best-achieved objective value among 10 runs are presented in column "Best objective". The "Avg-time" and "Avg-GAP" represent the average of computation times and the average of gaps, respectively. Column "*cache*" indicates the average percentage of cache usage in the HSCGA, while the "$eval$" represents the average number of evaluated fitness functions during the search. Table 3 confirms that HSCGA remarkably performs better than simple GA- LSFSN. The HSCGA provides 31% average savings by exerting cache table instead of recalculations. The results support that both HSCGA and FRDP are efficient methods for solving the problems.

Table 2. Performance of FRDP compared to the DP exact method for different examples of dataset 1

Instance	The deterministic model (TD-CITRM-DT)							The two-stage stochastic model (TD-CITRM-ST)						
	Dynamic programming (DP)		Flexible restricted dynamic programming (FRDP)					DP (RPAM)		FRDP (RPAM)				
	Obj.	Time (sec)	Settings	Best objective	$Acc-Sol$	Avg-time (sec)	Avg-GAP	Obj.	Time (sec)	Settings	Best objective	$Acc-Sol$	Avg-time (sec)	Avg-GAP
TD-CITRM_5_1	**82.43**	1.55	$\bar{H}$=10	**82.43**	10	1.41	0	**72.72**	1.74	$\bar{H}$=10	**72.72**	10	1.51	0
			$\bar{H}$=50	**82.43**	10	1.41	0			$\bar{H}$=50	**72.72**	10	1.60	0
			$\bar{H}$=500	**82.43**	10	1.43	0			$\bar{H}$=500	**72.72**	10	1.65	0
			$\bar{H}$=1500	**82.43**	10	1.43	0			$\bar{H}$=1500	**72.72**	10	1.65	0
			$\bar{H}$=5000	**82.43**	10	1.44	0			$\bar{H}$=5000	**72.72**	10	1.77	0
TD-CITRM_7_1	**100.47**	1.95	$\bar{H}$=10	**100.47**	10	1.47	0	**92.60**	2.71	$\bar{H}$=10	**92.60**	10	1.91	0
			$\bar{H}$=50	**100.47**	10	1.53	0			$\bar{H}$=50	**92.60**	10	2.21	0
			$\bar{H}$=500	**100.47**	10	1.81	0			$\bar{H}$=500	**92.60**	10	2.40	0
			$\bar{H}$=1500	**100.47**	10	1.89	0			$\bar{H}$=1500	**92.60**	10	2.60	0
			$\bar{H}$=5000	**100.47**	10	1.91	0			$\bar{H}$=5000	**92.60**	10	2.60	0
TD-CITRM_9_2	**110.83**	236.27	$\bar{H}$=10	122.14	10	1.81	0.102	**102.82**	339.1	$\bar{H}$=10	105.14	10	1.95	0.027
			$\bar{H}$=50	121.75	10	2.03	0.098			$\bar{H}$=50	105.14	10	2.33	0.022
			$\bar{H}$=500	115.11	10	4.45	0.038			$\bar{H}$=500	**102.82**	10	4.62	0
			$\bar{H}$=1500	115.11	10	8.24	0.038			$\bar{H}$=1500	**102.82**	10	8.13	0
			$\bar{H}$=5000	115.11	10	16.63	0.038			$\bar{H}$=5000	**102.82**	10	18.11	0
TD-CITRM_11_2	—	—	$\bar{H}$=10	×	×	×	×	—	—	$\bar{H}$=10	×	×	×	×
			$\bar{H}$=50	136.29	8	2.20	0.164			$\bar{H}$=50	119.25	10	2.51	0.066
			$\bar{H}$=500	132.02	10	7.41	0.126			$\bar{H}$=500	112.96	10	8.16	0.014
			$\bar{H}$=1500	128.59	10	15.33	0.101			$\bar{H}$=1500	112.96	10	16.1	0.009
			$\bar{H}$=5000	124.78	10	41.16	0.091			$\bar{H}$=5000	**111.85**	10	42.0	0
TD-CITRM_13_2	—	—	$\bar{H}$=10	×	×	×	×	—	—	$\bar{H}$=10	×	×	×	×
			$\bar{H}$=50	×	×	×	×			$\bar{H}$=50	×	×	×	×
			$\bar{H}$=500	148.89	10	11.03	0.182			$\bar{H}$=500	131.75	10	11.94	0.161
			$\bar{H}$=1500	142.58	10	26.61	0.158			$\bar{H}$=1500	131.75	10	28.52	0.156
			$\bar{H}$=5000	137.13	10	79.55	0.088			$\bar{H}$=5000	**122.21**	10	80.26	0.072
TD-CITRM_15_2	—	—	$\bar{H}$=10	×	×	×	×	—	—	$\bar{H}$=10	×	×	×	×
			$\bar{H}$=50	153.51	5	3.38	0.005			$\bar{H}$=50	×	×	×	×
			$\bar{H}$=500	147.62	10	16.19	0.002			$\bar{H}$=500	136.72	10	18.20	0.194
			$\bar{H}$=1500	147.34	10	43.37	0.0004			$\bar{H}$=1500	136.72	10	44.82	0.172
			$\bar{H}$=5000	**147.28**	10	125.0	0.0004			$\bar{H}$=5000	136.72	10	130.1	0.172
TD-CITRM_17_3	—	—	$\bar{H}$=10	×	×	×	×	—	—	$\bar{H}$=10	×	×	×	×
			$\bar{H}$=50	136.33	10	8.51	0.012			$\bar{H}$=50	134.59	10	14.04	0.071
			$\bar{H}$=500	136.33	10	34.72	0.010			$\bar{H}$=500	**125.59**	10	39.30	0
			$\bar{H}$=1500	136.18	10	116.91	0.008			$\bar{H}$=1500	**125.59**	10	121.41	0
			$\bar{H}$=5000	**134.98**	10	244.60	0			$\bar{H}$=5000	**125.59**	10	250.01	0
TD-CITRM_19_3	—	—	$\bar{H}$=10	×	×	×	×	—	—	$\bar{H}$=10	×	×	×	×
			$\bar{H}$=50	149.04	6	18.49	0.069			$\bar{H}$=50	134.52	8	25.19	0.005
			$\bar{H}$=500	146.48	10	58.72	0.031			$\bar{H}$=500	130.52	10	74.54	0.018
			$\bar{H}$=1500	146.48	10	132.72	0.031			$\bar{H}$=1500	130.52	10	146.52	0.015
			$\bar{H}$=5000	145.09	10	388.90	0.021			$\bar{H}$=5000	129.52	10	404.59	0.007
TD-CITRM_21_3	—	—	$\bar{H}$=10	×	×	×	×	—	—	$\bar{H}$=10	×	×	×	×
			$\bar{H}$=50	155.95	10	69.17	0.066			$\bar{H}$=50	139.18	6	87.16	0.037
			$\bar{H}$=500	152.99	10	105.08	0.046			$\bar{H}$=500	136.65	10	168.46	0.018
			$\bar{H}$=1500	149.92	10	202.71	0.024			$\bar{H}$=1500	135.42	10	255.86	0.011
			$\bar{H}$=5000	**146.22**	10	579.15	0.018			$\bar{H}$=5000	135.42	10	588.12	0.009
TD-CITRM_23_3	—	—	$\bar{H}$=10	×	×	×	×	—	—	$\bar{H}$=10	×	×	×	×
			$\bar{H}$=50	164.29	5	118.3	0.095			$\bar{H}$=50	144.71	4	268.12	0.041
			$\bar{H}$=500	160.18	10	244.7	0.067			$\bar{H}$=500	141.57	10	604.81	0.022
			$\bar{H}$=1500	160.18	10	409.3	0.067			$\bar{H}$=1500	141.57	10	1009.4	0.018
			$\bar{H}$=5000	158.63	10	1098.6	0.057			$\bar{H}$=5000	140.83	10	1596.2	0.013
TD-CITRM_25_3	—	—	$\bar{H}$=10	×	×	×	×	—	—	$\bar{H}$=10	×	×	×	×
			$\bar{H}$=50	×	×	×	×			$\bar{H}$=50	×	×	×	×
			$\bar{H}$=500	166.23	10	619.6	0.067			$\bar{H}$=500	148.16	10	1195.3	0.035
			$\bar{H}$=1500	166.23	10	882.1	0.067			$\bar{H}$=1500	148.16	10	1926.5	0.035
			$\bar{H}$=5000	163.17	10	1980.9	0.048			$\bar{H}$=5000	144.39	10	2446.7	0.026

Bold item: best-obtained solution

Table 3. Results obtained solving different examples of dataset 1 by HSCGA and simple GA-LSFSN

Instance	The deterministic model (TD-CITRM-DT)							
	HSCGA					Simple GA- LSFSN		
	Best objective	Avg-time (sec)	Avg-cache	*eval*	Avg-GAP	Best objective	Avg-time (sec)	Avg-GAP
TD-CITRM _5_1	**82.43**	2.68	0.99	24.0	0	**82.43**	4.04	0
TD-CITRM _7_1	**100.47**	3.23	0.95	710.0	0	**100.47**	9.53	0
TD-CITRM _9_2	**110.83**	7.91	0.66	6843.7	0	**110.83**	11.67	0.022
TD-CITRM _11_2	**118.06**	8.86	0.57	8942.0	0.017	**118.06**	13.36	0.029
TD-CITRM _13_2	**125.96**	9.87	0.54	9762.6	0.022	128.32	15.07	0.057
TD-CITRM _15_2	**147.28**	13.55	0.50	9397.9	0.015	150.01	18.04	0.119
TD-CITRM _17_3	136.18	19.87	0.48	9278.1	0.028	148.59	28.45	0.092
TD-CITRM _19_3	**142.06**	48.63	0.45	11134.7	0.054	150.01	57.07	0.122
TD-CITRM _21_3	**146.22**	183.9	0.40	11027.4	0.043	152.99	202.6	0.158
TD-CITRM _23_3	**150.00**	795.1	0.38	12016.4	0.054	**150.00**	869.2	0.232
TD-CITRM _25_3	**155.71**	1118.6	0.31	13108.6	0.062	160.18	1264.1	0.344
	The two-stage stochastic model (TD-CITRM-ST)							
Instance	HSCGA (RPAM)					Simple GA- LSFSN (RPAM)		
	Best objective	Avg-time (sec)	Avg-cache	*eval*	Avg-GAP	Best objective	Avg-time (sec)	Avg-GAP
TD-CITRM _5_1	**72.72**	2.74	0.99	24.0	0	**72.72**	8.52	0
TD-CITRM _7_1	**92.60**	3.41	0.95	701.6	0	**92.60**	10.02	0
TD-CITRM _9_2	**102.82**	8.14	0.66	6370.4	0	**102.82**	14.02	0.026
TD-CITRM _11_2	**111.85**	9.96	0.62	7348.6	0.022	114.06	16.78	0.031
TD-CITRM _13_2	**122.21**	10.28	0.52	9551.6	0.059	125.16	19.77	0.089
TD-CITRM _15_2	**116.59**	16.40	0.49	10026.1	0.035	143.06	23.96	0.129
TD-CITRM _17_3	127.41	26.94	0.46	10845.6	0.064	164.18	35.77	0.175
TD-CITRM _19_3	**128.52**	94.36	0.43	11004.7	0.082	140.18	112.2	0.159
TD-CITRM _21_3	**134.17**	382.46	0.38	12012.1	0.074	141.65	404.19	0.144
TD-CITRM _23_3	**140.69**	1015.9	0.34	12720.1	0.078	149.12	1086.9	0.220
TD-CITRM _25_3	**143.19**	1799.1	0.30	13514.0	0.088	153.16	1906.1	0.381

Bold item: best-obtained solution

Now, we evaluate the performance of RPAM strategy in comparison to bi-level optimization technique. To do this, the samples of dataset 1 are solved by FRDP and HSCGA. The results are reported in Table 4. In Table 4, the column "Diff" indicates the improvement of objective value in percentage induced by bi-level optimization technique. As expected, the computation times are increased significantly such that the examples with 23 and 25 nodes cannot be solved by this approach in reasonable times. However, the quality of stochastic solutions is on average 6.66% better than RPAM.

Table 4. Performance of bi-level optimization strategy versus RPAM for the examples of dataset 1

Instance	FRDP (Bi-level optimization method, $\bar{H}$=500)		HSCGA (Bi-level optimization method)		Best-found solution with RPAM strategy	Diff. (%)
	Best objective	Avg-time (sec)	Best objective	Avg-time (sec)		
TD-CITRM _5_1	**69.73**	1.94	**69.73**	3.512	72.72	4.28
TD-CITRM _7_1	**89.14**	5.613	**89.14**	7.051	92.60	3.88
TD-CITRM _9_2	**96.42**	119.87	**96.42**	179.18	102.82	6.63
TD-CITRM _11_2	104.30	233.71	**101.96**	255.16	111.85	9.69
TD-CITRM _13_2	106.73	564.36	**104.88**	664.70	122.21	16.52
TD-CITRM _15_2	115.49	804.53	**110.13**	980.62	116.59	5.86
TD-CITRM _17_3	**115.82**	1235.1	117.35	1404.6	125.59	8.43
TD-CITRM _19_3	127.48	3639.5	**125.71**	4112.7	128.52	2.23
TD-CITRM _21_3	**130.96**	12382.6	**130.96**	13074.0	134.17	2.45
TD-CITRM _23_3	×	×	×	×	140.69	×
TD-CITRM _25_3	×	×	×	×	143.19	×

Bold item: best-obtained solution

6.2.1 Evaluating the performance of FRDP

In this section, we evaluate the performance of the proposed FRDP in comparison to the RDP of Gromicho et al. (2012) and the RDP-DR of Tikani and Setak (2019). For this purpose, instances of dataset 1 are solved by the introduced methods with different restriction sizes as shown in Table 5.

Table 5. A comparison between the proposed FRDP with the classical RDP and RDP-DR for the examples of dataset 1 (OV: objective value, CT: computational time (in seconds), Inf: infeasible)

Instance		$H = 50$			$H = 500$			$H = 1{,}500$			$H = 5{,}000$		
		RDP	RDP-DR	FRDP	RDP	RDP-DR	FRDP	RDP	RDP-DR	FRDP	RDP	RDP-DR	FRDP
TD-CITRM_5_1	OV	82.43	82.43	82.43	82.43	82.43	82.43	82.43	82.43	82.43	82.43	82.43	82.43
	CT	1.54	1.48	1.41	1.66	1.50	1.43	1.69	1.54	1.43	1.74	1.58	1.44
	Gap	0	0	0	0	0	0	0	0	0	0	0	0
TD-CITRM_7_1	OV	100.47	100.47	100.47	100.47	100.47	100.47	100.47	100.47	100.47	100.47	100.47	100.47
	CT	1.72	1.66	1.53	2.09	2.07	1.81	2.14	2.10	1.89	2.22	2.13	1.91
	Gap	0	0	0	0	0	0	0	0	0	0	0	0
TD-CITRM_9_2	OV	128.61	124.41	121.75	124.41	121.75	115.11	121.75	115.11	115.11	115.11	115.11	115.11
	CT	2.13	2.11	2.03	5.36	4.92	4.45	11.06	11.44	9.24	22.01	18.82	16.63
	Gap	0.160	0.122	0.098	0.122	0.098	0.038	0.098	0.038	0.038	0.076	0.038	0.038
TD-CITRM_11_2	OV	Inf	Inf	136.29	135.86	136.29	132.02	139.56	134.92	130.05	132.71	130.04	128.59
	CT	×	×	2.20	8.31	7.67	7.41	20.05	19.81	15.33	48.70	46.43	41.16
	Gap	×	×	0.152	0.150	0.152	0.118	0.182	0.142	0.101	0.124	0.101	0.089
TD-CITRM_13_2	OV	Inf	Inf	Inf	154.7	154.7	148.89	154.7	148.89	142.58	148.89	148.89	137.13
	CT	×	×	×	18.64	16.87	11.03	28.03	25.39	26.61	85.53	76.01	79.55
	Gap	×	×	×	0.228	0.228	0.182	0.228	0.182	0.132	0.182	0.182	0.088
TD-CITRM_15_2	OV	Inf	Inf	153.51	153.51	153.51	147.62	147.62	153.51	147.34	147.62	147.62	147.28
	CT	×	×	3.38	15.21	13.18	16.19	41.16	33.46	43.37	118.54	122.18	125.0
	Gap	×	×	0.042	0.042	0.042	0.002	0.002	0.042	0.0004	0.002	0.002	0
TD-CITRM_17_3	OV	Inf	141.02	136.33	141.02	141.02	136.33	141.02	136.33	136.18	141.02	136.33	134.98
	CT	×	13.80	8.51	60.17	47.41	34.72	169.8	140.21	116.91	360.3	310.31	244.60
	Gap	×	0.044	0.01	0.044	0.044	0.01	0.044	0.01	0.008	0.044	0.01	0
TD-CITRM_19_3	OV	152.17	149.04	149.04	146.48	146.48	146.48	146.48	146.48	146.48	146.32	146.32	145.09
	CT	29.30	27.79	18.49	77.04	85.08	58.71	182.33	173.06	132.72	567.11	538.79	388.90
	Gap	0.071	0.049	0.049	0.031	0.031	0.031	0.031	0.031	0.031	0.030	0.030	0.021
TD-CITRM_21_3	OV	Inf	161.2	155.95	164.9	162.1	152.99	162.1	152.99	149.92	162.1	149.92	146.22
	CT	×	81.90	69.17	149.5	130.7	105.08	252.6	210.3	202.71	693.2	661.0	579.15
	Gap	×	0.102	0.066	0.127	0.108	0.046	0.108	0.046	0.025	0.108	0.025	0
TD-CITRM_23_3	OV	Inf	Inf	Inf	Inf	169.3	160.18	Inf	169.3	160.18	169.3	164.29	158.63
	CT	×	×	×	×	286.5	244.7	×	512.7	409.3	1,751.8	1,410.6	1,098.6
	Gap	×	×	×	×	0.128	0.067	×	0.128	0.067	0.128	0.095	0.057
TD-CITRM_25_3	OV	Inf	Inf	Inf	Inf	174.9	166.23	Inf	170.1	166.23	174.9	170.1	163.17
	CT	×	×	×	×	658.1	619.6	×	973.4	882.1	3,029.1	2,417.1	1,925.9
	Gap	×	×	×	×	0.123	0.067	×	0.092	0.067	0.123	0.092	0.092
Average	CT	8.65*	21.45*	13.34*	37.55*	114.0	100.46	78.76*	191.21	167.41	607.29	509.39	409.34
	Gap	0.057*	0.052*	0.056*	0.082*	0.086	0.051	0.077*	0.064	0.042	0.074	0.052	0.035

The sign (*) in the two last rows shows that the reported average values are calculated based on feasible runs

Based on the results obtained in Table 5, we can observe that FRDP provides competitive results in terms of solution times. Moreover, the obtained objective values are not much far from the ones provided in other published studies.

6.3 The advantage of multigraph representation

The proposed CIT transportation models allowed employing parallel links for designing a safe and efficient routing scheme. In addition to traffic congestion, the risk of traveling affects the link selection in the routing plan. Let us evaluate the achievement of using multigraph via simple graph by the criteria Improvement(%) = $\frac{|\mathcal{OBJ}^M - \mathcal{OBJ}^S|}{\mathcal{OBJ}^S} \times 100\%$ where $\mathcal{OBJ}^M$ and $\mathcal{OBJ}^S$ represent the objective function of the problem in the multigraph and simple graph, respectively. Here, we investigate the significance of considering parallel arcs between demand nodes in different size instances of dataset 1. Similar to Tikani and Setak (2019), we change the multigraph network to simple network to obtain the corresponding $\mathcal{OBJ}^S$ by randomly selecting one link between each pair of nodes. The results of comparing the objective functions of multigraph versus simple graph representations are exhibited in Table 6.

Table 6. Comparing the objective function of multigraph and simple graph in TD-CITRM-ST

Instance	Multigraph	Simple graph	Improvement %
TD-CITRPM_7_1	100.47	108.28	7.21
TD-CITRPM_11_2	118.06	133.43	11.5
TD-CITRPM_15_2	147.28	164.00	10.2
TD-CITRPM_19_3	142.06	156.28	9.09
TD-CITRPM_23_3	150.00	171.23	12.3
Average			10.06

From Tables 6, it comes out that multigraph network can have substantial effects on the quality of solutions in the proposed problem. In these examples, using a multigraph helps to decrease the objective function 10.06% in average.

6.4 Value of the stochastic TD-CITRM-ST

To examine the potential benefit of solving the stochastic TD-CITRM-ST over solving the deterministic TD-CITRM-DT, we evaluated two well-known concepts named EVPI and VSS (Birge and Louveaux 2011). In what follows, we define the wait-and-see value and then related formulations of EVPI and VSS are presented. Consider ω as a random variable whose realizations relate to different scenarios. Let $\mathcal{OBJ}^*$ defined as the optimal value of the stochastic programming, and $\overline{\mathcal{OBJ}}(\omega)$ stands for the optimal value of the deterministic version of the problem for one specific scenario $\omega \in \Omega$.

Wait-and-see (WS): this value represents the expected value of the objective function for each scenario $\omega \in \Omega$, which is computed by $WS = E_\omega(\overline{\mathcal{OBJ}}(\omega))$.

Expected Value of Perfect Information (EVPI): this concept denotes the maximum amount that should be paid by decision makers in return of getting information about the future. The EVPI is obtained by $EVPI = WS - \mathcal{OBJ}^*$.

Expected of Expected Value (EEV): To achieve EEV-Solution first the stochastic parameters are replaced by their corresponding expected values. Then the deterministic model is solved and evaluated for all scenarios. If $\bar{Z}(\bar{\omega})$ presents the optimal decision in the first stage of the deterministic model, the EEV becomes $EEV = E_\omega(\mathcal{OBJ}(\bar{Z}(\bar{\omega}), \omega))$.

Value of the Stochastic Solution (VSS): The VSS measures that whether modeling and computational solving efforts on stochastic programming is worthwhile. It equals the difference between EEV and the optimal value of the stochastic programming ($VSS = \mathcal{OBJ}^* - EEV$). The lower value of VSS implies that applying the expected values of random variables as an approximation for uncertain input parameters is a suitable option. Conversely, the higher value shows the advantages of employing stochastic programming method (for complete information we refer the reader to Birge and Louveaux, 2011).

We compute the discussed indexes for the TD-CITRM-ST using dataset 1 in Table 7. It contains the relative $EVPI$ and VSS in percentage. It can be seen from Table 7 that in the studied problems, the range of relative EVPI is from 0.94% to 3.61%, while the range of relative VSS is from 2.23% to 8.84%. Moreover, the average relative EVPI=2.40% is less than the average relative VSS=5.20%. The results imply that the knowledge about the traffic speeds is relatively important; however, having such information in practice is very difficult. The information of

Table 7 about VSS indicates that it is certainly worth to put extra effort in modeling and solving the stochastic problem.

Table 7. Values of VSS and EVPI for TD-CITRM-ST

Instance	$\mathcal{OBj}^*$	WS	Relative EVPI (%)	EEV	Relative VSS (%)
TD-CITRPM_7_1	89.14	88.30	0.94	92.60	3.88
TD-CITRPM_11_2	101.96	99.42	2.49	111.85	8.84
TD-CITRPM_15_2	110.13	107.28	2.58	116.59	5.86
TD-CITRPM_19_3	125.71	121.17	3.61	128.52	2.23
Average			2.40		5.20

6.5 Managerial insights

This paper provides important suggestions for practitioners in CIT companies. In this sector, the operations are perpetually exposed to the risk of robberies. Herein, we studied new models for cash transportation to consider more actual factors in inter-city roads. The following managerial insights can be extracted from this study:

i. Our results indicate that multigraph representation certainly improves the routing plans in CIT sector. The reason behind this fact is that multigraph setting keeps all non-dominated links between nodes. In overall, when the links have several attributes (e.g., risk, time), multigraphs should be employed to consider trade-offs between the defined attributes. In this regard, we observed the average savings in the objectives ranged from 4% to 12% in the real case study and other generated instances.
ii. Discarding the traffic congestion patterns leads to imprecisions in routing decisions of CIT companies. High traffic condition not only increases the total operation time but also affects the risk of exposure. In particular, time-varying traffic congestion influences both appropriate link between nodes and starting time of carrier operation.
iii. From a CIT company's perspective, it is favorable to provide balanced carrier operations in which the routing plans are accomplished in a certain time. On the other hand, the economic organizations generally tend to accelerate the cash carrier operation to gain higher customer service level. To this end, the proposed models guarantee that all routes are completed before a given time. This trait not only plays a significant role in CIT operations but also helps to provide a sufficient inventory of banknotes for the customers at the right time.
iv. Planning CIT routes without taking the vehicles' speed uncertainty into account may result in poor quality solutions. Since the traffic conditions are not necessarily known in advance, incorporating variability in the speed patterns yields to achieve robust solutions. The comparisons between the stochastic solutions and deterministic counterpart justified the use of sophisticated modeling approaches and extra computational challenges.

7. Conclusions

In this paper, we have formulated a risk-constrained time-dependent VRP for the transportation of physical currency. This study explicitly strives to fill the gap in the relevant literature by:

(i) employing multigraph representation in routing plans of CIT sector,
(ii) investigating the problem under both deterministic and stochastic time-varying traffic congestion. Ignoring the concept of traffic congestions in CIT transportation may bring imprecise decisions in such problems.
(iii) introducing a new risk index that captures the existence of parallel links with different traffic congestions,
(iv) designing a more balanced routing scheme by imposing maximum duration time together with a risk threshold for each constructed route.

Multigraph networks keep all efficient parallel links between each pair of nodes. Here, the parallel links are distinguished by two attributes including time-varying travel time (which adheres FIFO property) and traveling risk. Obviously, both features affect the routing plan. For example, due to the traffic congestion passing an alternative longer link can be faster and can save time. In another case, the model may choose a safer link to

mitigate the total transportation risk. The computational comparisons showed that multigraph representation could improve the objective value by preserving non-dominated parallel links in the solution space. In overall, considering flexibility in selecting the links is a significant factor in time-critical logistics in city configurations.

Presenting efficient solution methods for the proposed models is extremely challenging. Because the optimization process not only determines the delivery sequence but also should give the candidate links among them. In this respect, we provided efficient methods including dynamic programming (exact method), a flexible restricted dynamic programming (heuristic based method), and hybrid self-adaptive caching genetic algorithm (metaheuristic method) to solve the problem. The LSFSN algorithm is embedded in each algorithm to explore the links and choose proper ones. The LSFSN benefits from dominance mechanism and feasibility rules to decrease the cardinality in searching. Afterward, the methods are adapted to handle the uncertain parameters by two strategies: bi-level optimization process and Route-Path approximation method. We analyzed the structure of solutions and objective values of TD-CITRM-DT and TD-CITRM-ST by the mentioned algorithms. The observations implied that the stochastic solutions are better than the deterministic version but solving two-stage stochastic program needs extra computational efforts. Finally, to show the applicability of the model, the problem was implemented on a CIT company in Isfahan metropolis as a case study.

Interesting directions for future researches are investigating the trade-off between travel time and risk of transportation using multi-objective optimization methods; inspired by Hoogeboom, and Dullaert (2019), incorporating the time windows with prohibition of waiting times; considering multi-period planning or precedence constraints in the models and presenting more efficient algorithms to solve the stochastic version of the problem.

Appendix A. List of notations

Table A.1. Notation and definitions

Notation	Description	First appeared section
N	Set of demand nodes $N = \{1, \dots, n\}$	3
P	Depot node and its copy $P = \{0 \cup n+1\}$	3
i, j	Indices to nodes $i, j \in (N \cup P)$	3
K	Set of vehicles indexed by $k \in \{1, \dots, \lvert K \rvert\}$	3
M_{ij}	Set of available traffic links from node i to node j, $i \neq j$ indexed by $m \in \{1, \dots, \lvert M_{ij} \rvert\}$	3
D_i	The demand at location i	3
s_i	Service time for serving demand node i	3
Q	Capacity of a vehicle	3
ρ	Maximum allowable cumulative risk for each vehicle (risk threshold value)	3
δ	Maximum allowable expected en-route time for each vehicle	3
Tr_{ij}^{m}	The probability (threat) of robbery happening in the mth link from node i to node j per unit of time	3
H_m	Set of time intervals in the mth edge between two sequential nodes indexed by $h \in \{1, \dots, \lvert H_m \rvert\}$	3.1
a_{ijm}^{h}, b_{ijm}^{h}	Coefficients for determining the travel time in the mth edge from node i to node j	3.1
$\bar{T}_{ijm}^{h}$	The head points of new time intervals in the mth edge from node i to node j	3.1
t_i^k	Departure time of the vehicle k from node i	3.3
r_{ijm}^{k}	The risk of robbery occurrence on a link (i, j, m) passed by the vehicle k	3.3
v_{ijm}	Vulnerability factor for the mth edge from node i to node j	3.3
Cp_i^k	The remaining valuable goods at node i for the vehicle k	3.3
R_i^k	The cumulative risk at node i for the vehicle k	3.3
x_{ij}^{k}	Equal to 1 if the vehicle k goes from node i to node j	4.2

x_{ijm}^{hk}	Equal to 1 if the vehicle k moves through the mth edge from node i to node j in the hth time interval	4.2
E	A large constant number	4.2
Ω	Set of scenarios $\omega \in \Omega$	4.3
y_{im}^{h}	Equal to 1 if the mth link from node i to its corresponding successor node is selected in the hth time interval (for LSFSN)	5.1.3
t_i	Departure time of the vehicle at node i (for LSFSN)	5.1.3
R_i	The cumulative risk at node i (for LSFSN)	5.1.3
Cp_i	The remaining valuable goods at node i (for LSFSN)	5.1.3

Appendix B. Characteristics of test problems

To investigate the limitations of the proposed mathematical models in relation to the problem size, we produced additional numerical examples in multigraph networks. To do this, three datasets with variability in time intervals, demands, and service time are generated where the nodes are connected to each other by multiple parallel links. Then, the proposed models are implemented on subsets of each generated dataset by considering the first N number of nodes participating in the multigraph.

Table B.1 represents the information of each demand node on each dataset. The demands of dataset 1 are generated by discrete uniform distribution $\{DU(1,10) \times 10\}$, and for datasets 2 & 3 the assigned demand to each node is multiplied by 2 and 3, respectively. Length of the shorter link (with the higher congestion) between two nodes i and j is a multiple of Euclidean distance ED_{ij}, while, the length of the alternative longer link is generated by uniform function $U[1.1 \times ED_{ij}, 1.5 \times ED_{ij}]$. Then the procedure of Section 3.1 is employed to calculate the time-dependent travel time between the nodes. In this regard, the links are categorized into two groups based on their traffic congestions. The first group represents the shorter links with the high-traffic condition while the second alternative links are longer than the first one but the speeds are less dependent to the changes of time intervals (it represents the low-traffic alternative links). The speeds of TD-CITRM-ST are assigned in the interval of [35, 75] and two scenarios are considered with respective probabilities of 60% and 40%. Whereas, for TD-CITRM-DT, the average of all traffic speeds according to their respective probabilities is considered as traffic speeds in different time-intervals by $v_{Deterministic} = (0.6 \times v_{\text{Scenario I}}) + (0.4 \times v_{\text{Scenario II}})$. The details of speed patterns for three datasets are listed in Table B.2. Furthermore, three states of high/medium/low are considered for the robbery risk per unit of time in the available links. For this purpose, the robbery risk per unit of time is set to 0.01, 0.006, and 0.002, randomly. For dataset 1, the maximum time duration and risk threshold for examples TD-CITRM _5_1 to TD-CITRM _15_2 are set to 110 and 60, respectively. For the rest of the examples, these values are set to 150 and 90, respectively. For dataset 2 & 3 the aforementioned values and the capacity of vehicles are multiplied by 0.5 and 1.5, respectively. Finally, the duration of service time for datasets 1 and 2 are set to 1, while in the dataset 3, an integer service time in {1, 2} was randomly assigned to each demand node.

Table B.1. Characteristics of demand nodes in the test problems

# Node	Nodes' locations		Dataset #1		Dataset #2		Dataset #3	
	x_ coordinate	y_ coordinate	Demand	Service time	Demand	Service time	Demand	Service time
1 (depot)	100	100	0	0	0	0	0	0
2	181	172	40	1	80	1	120	1
3	154	31	90	1	180	1	270	1
4	123	106	90	1	180	1	270	2
5	23	137	80	1	160	1	240	1
6	190	28	10	1	200	1	30	1
7	8	71	80	1	160	1	240	2
8	103	130	50	1	100	1	150	1
9	62	50	60	1	120	1	180	1
10	89	161	40	1	80	1	120	1
11	117	91	60	1	120	1	180	1
12	12	156	60	1	120	1	180	2
13	88	165	30	1	60	1	90	2
14	107	125	80	1	160	1	240	1
15	8	74	60	1	120	1	180	1
16	105	125	90	1	180	1	270	2
17	118	192	30	1	60	1	90	1
18	146	11	10	1	20	1	30	1
19	93	13	60	1	120	1	180	1
20	188	125	50	1	100	1	150	2
21	87	117	10	1	20	1	30	1
22	123	31	80	1	160	1	240	2
23	121	189	70	1	140	1	210	1
24	174	128	10	1	20	1	30	1
25	197	80	30	1	60	1	90	1

Table B.2. Speed pattern for the test problems

	Time interval	Scenario I		Scenario II		Deterministic	
		Low traffic	High traffic	Low traffic	High traffic	Low traffic	High traffic
Dataset #1	[0-3]	65	55	60	45	63	51
	[3-6]	60	45	50	40	56	43
	[6-10]	62	50	42	35	45	44
Dataset #2	[0-2]	66	59	61	49	64	55
	[2-4]	60	57	55	47	58	53
	[6-8]	58	54	53	44	56	50
	[8-10]	62	56	57	46	60	52
Dataset #3	[0-5]	72	65	67	55	70	61
	[5-10]	68	56	58	51	64	54

Appendix C. Detailed solution values for dataset 2 & 3

Tables C.1 and C.2 report the detailed results of HSCGA and simple GA-LSFSN on each subset of 2 and dataset 3. In addition, the performance of the proposed DP and FRDP for these datasets are listed in Table C.3 and Table C.4. For each instance, the best obtained objective value is highlighted in boldface.

Table C.1. The results of solving different examples by HSCGA and simple GA-LSFSN for dataset 2

The deterministic model (TD-CITRM-DT)								
Instance	HSCGA					Simple GA- LSFSN		
	Best objective	Avg-time (sec)	Avg-cache	*eval*	Avg-GAP	Best objective	Avg-time (sec)	Avg-GAP
TD-CITRM _5_1	**75.53**	4.50	0.99	25.0	0	**75.53**	5.92	0
TD-CITRM _7_1	**94.56**	6.01	0.95	712.4	0	**94.56**	7.51	0
TD-CITRM _9_2	**103.37**	9.49	0.64	6665.8	0	**103.37**	10.82	0.027
TD-CITRM _11_2	**109.24**	11.72	0.55	8630.5	0.019	**109.24**	14.67	0.029
TD-CITRM _13_2	**120. 91**	14.68	0.54	9764.8	0.023	**120. 91**	19.04	0.056
TD-CITRM _15_2	**129.69**	21.99	0.51	9589.2	0.022	136.43	30.68	0.120
TD-CITRM _17_3	120.72	33.74	0.47	9089.7	0.030	120.72	48.71	0.123
TD-CITRM _19_3	**123.32**	62.23	0.43	10647.3	0.051	**123.32**	79.05	0.125
TD-CITRM _21_3	**134.14**	201.81	0.40	11038.1	0.047	140.17	288.56	0.155
TD-CITRM _23_3	**136.72**	849.62	0.35	11091.8	0.057	152.09	1197.03	0.243
TD-CITRM _25_3	**148.15**	1309.42	0.30	12770.2	0.069	163.08	1508.41	0.313
The two-stage stochastic model (TD-CITRM-ST)								
Instance	HSCGA (RPAM)					Simple GA- LSFSN (RPAM)		
	Best objective	Avg-time (sec)	Avg-cache	*eval*	Avg-GAP	Best objective	Avg-time (sec)	Avg-GAP
TD-CITRM _5_1	**62.50**	5.08	0.99	24.0	0	**62.50**	7.01	0
TD-CITRM _7_1	**84.47**	7.27	0.95	710.1	0	**84.47**	9.52	0
TD-CITRM _9_2	**93.07**	10.95	0.65	6783.2	0	**93.07**	15.2	0.033
TD-CITRM _11_2	**99.47**	14.54	0.62	7560.1	0.036	**99.47**	18.91	0.032
TD-CITRM _13_2	**110.61**	17.83	0.51	9706.5	0.061	115.93	26.20	0.077
TD-CITRM _15_2	**113.19**	29. 32	0.49	10038.2	0.055	117.06	37.34	0.119
TD-CITRM _17_3	**109. 35**	48.25	0.47	10040.0	0.068	114.10	56.85	0.154
TD-CITRM _19_3	121. 11	102.62	0.44	10857.8	0.078	130.51	154.06	0.163
TD-CITRM _21_3	**119.87**	418.76	0.39	11972.5	0.081	137.25	572. 59	0.172
TD-CITRM _23_3	**125.01**	1346.83	0.33	11910.4	0.077	140.11	1491. 73	0.262
TD-CITRM _25_3	**135.14**	1998.06	0.29	13970.1	0.089	157.23	2152.86	0.376

Table C.2. The results of solving different examples by HSCGA and simple GA-LSFSN for dataset 3

The deterministic model (TD-CITRM-DT)								
Instance	HSCGA					Simple GA- LSFSN		
	Best objective	Avg-time (sec)	Avg-cache	*eval*	Avg-GAP	Best objective	Avg-time (sec)	Avg-GAP
TD-CITRM _5_1	**65.31**	2.60	0.99	25.0	0	**65.31**	3.95	0
TD-CITRM _7_1	**83.62**	2.77	0.95	712.4	0	**83.62**	7.51	0
TD-CITRM _9_2	**87.83**	6.47	0.63	6687.4	0	**87.83**	10.03	0.019
TD-CITRM _11_2	**95.65**	7.59	0.58	8215.3	0.018	**95.65**	12.82	0.030
TD-CITRM _13_2	**102.02**	8.35	0.55	9509.1	0.020	104.02	15.00	0.047
TD-CITRM _15_2	**112.58**	11.62	0.51	9601.8	0.018	117.23	19.85	0.091
TD-CITRM _17_3	**97.72**	16.85	0.46	9703.7	0.033	106.12	24.91	0.103
TD-CITRM _19_3	**107.14**	40.46	0.44	11017.2	0.046	115.80	48.60	0.116
TD-CITRM _21_3	**114.71**	159.13	0.40	11764.7	0.044	132.95	184.31	0.153
TD-CITRM _23_3	**116.86**	690.05	0.36	11568.8	0.057	140.12	712.62	0.226
TD-CITRM _25_3	**126.30**	964.31	0.29	12543.1	0.063	159.01	1010.71	0.319
The two-stage stochastic model (TD-CITRM-ST)								
Instance	HSCGA (RPAM)					Simple GA- LSFSN (RPAM)		
	Best objective	Avg-time (sec)	Avg-cache	*eval*	Avg-GAP	Best objective	Avg-time (sec)	Avg-GAP
TD-CITRM _5_1	**56.13**	2.32	0.99	25.0	0	**56.13**	5.01	0
TD-CITRM _7_1	**75.22**	2.09	0.95	710.1	0	**75.22**	9.43	0
TD-CITRM _9_2	**82.32**	6.26	0.65	6783.2	0	**82.32**	13.20	0.023
TD-CITRM _11_2	**84.12**	8.97	0.60	7871.0	0.022	**84.12**	15.50	0.033
TD-CITRM _13_2	**96.87**	9.32	0.53	9671.5	0.031	107.02	18.04	0.064
TD-CITRM _15_2	**101.03**	13.58	0.50	9902.9	0.052	113.10	21.14	0.114
TD-CITRM _17_3	**88.50**	23.16	0.47	10040.0	0.061	92.49	30.76	0.122
TD-CITRM _19_3	105.03	79.78	0.44	10962.3	0.069	110.57	90.22	0.133
TD-CITRM _21_3	**108.09**	327.46	0.41	11053.4	0.074	119.05	370. 0	0.172
TD-CITRM _23_3	**111.33**	886.47	0.34	11521.4	0.087	129.31	897. 63	0.264

TD-CITRM _25_3	**119.18**	1572.64	0.29	13061.1	0.081	137.64	1620.12	0.372							

Table C.3. The results of implementing FRDP and the DP exact method for different examples of dataset 2

Instance	The deterministic model (TD-CITRM-DT)							The two-stage stochastic model (TD-CITRM-ST)							
	Dynamic programming (DP)		Flexible restricted dynamic programming (FRDP)					DP (RPAM)		FRDP (RPAM)					
	Obj.	Time (sec)	Settings	Best objective	$Acc-Sol$	Avg-time (sec)	GAP	Obj.	Time (sec)	Settings	Best objective	$Acc-Sol$	Avg-time (sec)	GAP
TD-CITRM _5_1	**62.50**	1.85	$\bar{H}$=10	**75.53**	10	1.71	0	**62.50**	1.97	$\bar{H}$=10	**62.50**	10	1.78	0
			$\bar{H}$=50	**75.53**	10	1.71	0			$\bar{H}$=50	**62.50**	10	1.78	0
			$\bar{H}$=500	**75.53**	10	1.74	0			$\bar{H}$=500	**62.50**	10	1.78	0
			$\bar{H}$=1500	**75.53**	10	1.74	0			$\bar{H}$=1500	**62.50**	10	1.80	0
			$\bar{H}$=5000	**75.53**	10	1.78	0			$\bar{H}$=5000	**62.50**	10	1.88	0
TD-CITRM _7_1	**94.56**	2.41	$\bar{H}$=10	**94.56**	10	1.69	0	**84.47**	4.03	$\bar{H}$=10	**92.60**	10	2.57	0
			$\bar{H}$=50	**94.56**	10	1.73	0			$\bar{H}$=50	**92.60**	10	2.71	0
			$\bar{H}$=500	**94.56**	10	1.94	0			$\bar{H}$=500	**92.60**	10	2.95	0
			$\bar{H}$=1500	**94.56**	10	2.09	0			$\bar{H}$=1500	**92.60**	10	3.07	0
			$\bar{H}$=5000	**94.56**	10	2.25	0			$\bar{H}$=5000	**92.60**	10	3.91	0
TD-CITRM _9_2	**103.37**	275.09	$\bar{H}$=10	113.54	10	3.02	0.098	**93.07**	374.5	$\bar{H}$=10	99.72	10	4.42	0.071
			$\bar{H}$=50	108.05	10	4.51	0.045			$\bar{H}$=50	95.15	10	5.13	0.022
			$\bar{H}$=500	105.17	10	6.75	0.033			$\bar{H}$=500	95.15	10	8.05	0
			$\bar{H}$=1500	105.17	10	11.04	0.027			$\bar{H}$=1500	**93.07**	10	14.12	0
			$\bar{H}$=5000	**103.37**	10	21.81	0.027			$\bar{H}$=5000	**93.07**	10	25.84	0
TD-CITRM _11_2	_	_	$\bar{H}$=10	×	×	×	×	_	_	$\bar{H}$=10	×	×	×	×
			$\bar{H}$=50	114.95	9	5.64	0.055			$\bar{H}$=50	105.40	10	6.01	0.059
			$\bar{H}$=500	112.07	10	10.29	0.125			$\bar{H}$=500	101.21	10	12.72	0.025
			$\bar{H}$=1500	112.07	10	20.02	0.025			$\bar{H}$=1500	101.21	10	24.11	0.017
			$\bar{H}$=5000	**109.24**	10	46.23	0			$\bar{H}$=5000	100.17	10	49.02	0.017
TD-CITRM _13_2	_	_	$\bar{H}$=10	×	×	×	×	_	_	$\bar{H}$=10	×	×	×	×
			$\bar{H}$=50	×	×	×	×			$\bar{H}$=50	×	×	×	×
			$\bar{H}$=500	137.19	10	16.75	0.134			$\bar{H}$=500	114.60	10	19.14	0.036
			$\bar{H}$=1500	130.17	10	31.10	0.076			$\bar{H}$=1500	111.54	10	34.87	0.019
			$\bar{H}$=5000	**120.91**	10	83.05	0.024			$\bar{H}$=5000	**110.61**	10	88.60	0.003
TD-CITRM _15_2	_	_	$\bar{H}$=10	×	×	×	×	_	_	$\bar{H}$=10	×	×	×	×
			$\bar{H}$=50	140.65	6	8.20	0.084			$\bar{H}$=50	124.08	3	×	0.096
			$\bar{H}$=500	140.65	10	22.54	0.084			$\bar{H}$=500	120.12	10	26.91	0.074
			$\bar{H}$=1500	136.50	10	51.19	0.058			$\bar{H}$=1500	120.12	10	54.12	0.061
			$\bar{H}$=5000	136.50	10	142.4	0.052			$\bar{H}$=5000	120.12	10	150.7	0.061
TD-CITRM _17_3	_	_	$\bar{H}$=10	×	×	×	×	_	_	$\bar{H}$=10	×	×	×	×
			$\bar{H}$=50	121.29	9	15.22	0.012			$\bar{H}$=50	118.74	9	24.82	0.085
			$\bar{H}$=500	121.29	10	47.80	0.010			$\bar{H}$=500	110.19	10	53.05	0.007
			$\bar{H}$=1500	**119.05**	10	130.1	0.008			$\bar{H}$=1500	**109.35**	10	137.0	0049
			$\bar{H}$=5000	**119.05**	10	274.3	0			$\bar{H}$=5000	**109.35**	10	300.2	0
TD-CITRM _19_3	_	_	$\bar{H}$=10	×	×	×	×	_	_	$\bar{H}$=10	×	×	×	×
			$\bar{H}$=50	130.05	7	28.07	0.054			$\bar{H}$=50	130.63	7	34.19	0.110
			$\bar{H}$=500	127.68	10	63.24	0.035			$\bar{H}$=500	123.12	10	80.02	0.046
			$\bar{H}$=1500	124.25	10	152.8	0.015			$\bar{H}$=1500	121.11	10	166.5	0.029
			$\bar{H}$=5000	**123.32**	10	397.1	0.007			$\bar{H}$=5000	**117.63**	10	415.9	0.011
TD-CITRM _21_3	_	_	$\bar{H}$=10	×	×	×	×	_	_	$\bar{H}$=10	×	×	×	×
			$\bar{H}$=50	145.95	8	80.41	0.088			$\bar{H}$=50	130.09	7	97.22	0.085
			$\bar{H}$=500	136.42	10	154.2	0.016			$\bar{H}$=500	126.62	10	206.4	0.056
			$\bar{H}$=1500	135.19	10	219.0	0.013			$\bar{H}$=1500	122.47	10	271.8	0.011
			$\bar{H}$=5000	**134.14**	10	601.1	0.002			$\bar{H}$=5000	**119.87**	10	630.7	0.003
TD-CITRM _23_3	_	_	$\bar{H}$=10	×	×	×	×	_	_	$\bar{H}$=10	×	×	×	×
			$\bar{H}$=50	149.09	5	134.6	0.090			$\bar{H}$=50	135.05	3	295.0	0.080
			$\bar{H}$=500	140.23	10	304.1	0.063			$\bar{H}$=500	135.05	10	631.4	0.080
			$\bar{H}$=1500	140.23	10	431.2	0.063			$\bar{H}$=1500	128.17	10	1102.5	0.025
			$\bar{H}$=5000	**136.72**	10	1203.5	0.012			$\bar{H}$=5000	126.44	10	1668.1	0.011
TD-CITR	_	_	$\bar{H}$=10	×	×	×	×	_	_	$\bar{H}$=10	×	×	×	×
			$\bar{H}$=50	×	×	×	×			$\bar{H}$=50	×	×	×	×
			$\bar{H}$=500	158.41	10	702.0	0.069			$\bar{H}$=500	146.75	10	1304.2	0.085

			$\bar{H}$=1500	154.41	10	1012.4	0.047			$\bar{H}$=1500	142.33	10	2103.1	0.031
			$\bar{H}$=5000	149.32	10	2250.1	0.031			$\bar{H}$=5000	137.25	10	2871.0	0.069

Table C.4. The results of implementing FRDP and the DP exact method for different examples of dataset 3

Instance	The deterministic model (TD-CITRM-DT)							The two-stage stochastic model (TD-CITRM-ST)							
	Dynamic programming (DP)		Flexible restricted dynamic programming (FRDP)					DP (RPAM)		FRDP (RPAM)					
	Obj.	Time (sec)	Settings	Best objective	$Acc-Sol$	Avg-time (sec)	Avg-GAP	Obj.	Time (sec)	Settings	Best objective	$Acc-Sol$	Avg-time (sec)	Avg-GAP
TD-CITRM_5_1	**65.31**	1.47	$\bar{H}$=10	**65.31**	10	1.39	0	**56.13**	1.74	$\bar{H}$=10	**56.13**	10	1.43	0
			$\bar{H}$=50	**65.31**	10	1.39	0			$\bar{H}$=50	**56.13**	10	1.43	0
			$\bar{H}$=500	**65.31**	10	1.43	0			$\bar{H}$=500	**56.13**	10	1.45	0
			$\bar{H}$=1500	**65.31**	10	1.43	0			$\bar{H}$=1500	**56.13**	10	1.45	0
			$\bar{H}$=5000	**65.31**	10	1.45	0			$\bar{H}$=5000	**56.13**	10	1.63	0
TD-CITRM_7_1	**83.62**	1.95	$\bar{H}$=10	**83.62**	10	1.45	0	**75.22**	2.71	$\bar{H}$=10	**75.22**	10	1.75	0
			$\bar{H}$=50	**83.62**	10	1.50	0			$\bar{H}$=50	**75.22**	10	2.09	0
			$\bar{H}$=500	**83.62**	10	1.72	0			$\bar{H}$=500	**75.22**	10	2.23	0
			$\bar{H}$=1500	**83.62**	10	1.80	0			$\bar{H}$=1500	**75.22**	10	2.44	0
			$\bar{H}$=5000	**83.62**	10	1.86	0			$\bar{H}$=5000	**75.22**	10	2.44	0
TD-CITRM_9_2	**87.83**	236.27	$\bar{H}$=10	100.75	10	1.71	0.147	**82.32**	339.1	$\bar{H}$=10	98.17	10	1.84	0.192
			$\bar{H}$=50	100.75	10	1.91	0.147			$\bar{H}$=50	98.17	10	2.11	0.192
			$\bar{H}$=500	94.19	10	3.85	0.072			$\bar{H}$=500	86.12	10	4.05	0.046
			$\bar{H}$=1500	94.19	10	7.19	0.072			$\bar{H}$=1500	86.12	10	7.53	0.046
			$\bar{H}$=5000	**87.83**	10	14.13	0			$\bar{H}$=5000	86.12	10	15.19	0.046
TD-CITRM_11_2	—	—	$\bar{H}$=10	×	×	×	×	—	—	$\bar{H}$=10	×	×	×	×
			$\bar{H}$=50	112.50	7	2.10	0.176			$\bar{H}$=50	104.80	7	2.38	0.245
			$\bar{H}$=500	112.50	10	6.01	0.176			$\bar{H}$=500	90.32	10	7.20	0.073
			$\bar{H}$=1500	103.05	10	13.04	0.077			$\bar{H}$=1500	87.22	10	15.34	0.036
			$\bar{H}$=5000	99.64	10	36.51	0.041			$\bar{H}$=5000	**84.12**	10	39.11	0.010
TD-CITRM_13_2	—	—	$\bar{H}$=10	×	×	×	×	—	—	$\bar{H}$=10	×	×	×	×
			$\bar{H}$=50	×	×	×	×			$\bar{H}$=50	×	×	×	×
			$\bar{H}$=500	118.72	10	9.71	0.163			$\bar{H}$=500	105.60	10	10.01	0.090
			$\bar{H}$=1500	110.28	10	22.56	0.080			$\bar{H}$=1500	105.60	10	26.02	0.090
			$\bar{H}$=5000	**102.02**	10	74.01	0.024			$\bar{H}$=5000	**96.87**	10	77.90	0.036
TD-CITRM_15_2	—	—	$\bar{H}$=10	×	×	×	×	—	—	$\bar{H}$=10	×	×	×	×
			$\bar{H}$=50	120.17	6	3.19	0.067			$\bar{H}$=50	×	×	×	×
			$\bar{H}$=500	117.02	10	14.00	0.039			$\bar{H}$=500	116.21	10	16.91	0.150
			$\bar{H}$=1500	117.02	10	36.20	0.039			$\bar{H}$=1500	116.21	10	38.18	0.150
			$\bar{H}$=5000	**112.58**	10	116.5	0.011			$\bar{H}$=5000	109.64	10	121.0	0.085
TD-CITRM_17_3	—	—	$\bar{H}$=10	×	×	×	×	—	—	$\bar{H}$=10	×	×	×	×
			$\bar{H}$=50	104.51	10	6.76	0.069			$\bar{H}$=50	101.09	10	10.13	0.142
			$\bar{H}$=500	104.51	10	29.02	0.069			$\bar{H}$=500	96.21	10	36.74	0.093
			$\bar{H}$=1500	101.20	10	101.13	0.051			$\bar{H}$=1500	**88.50**	10	107.40	0.034
			$\bar{H}$=5000	101.20	10	227.20	0.035			$\bar{H}$=5000	**88.50**	10	235.91	0
TD-CITRM_19_3	—	—	$\bar{H}$=10	×	×	×	×	—	—	$\bar{H}$=10	×	×	×	×
			$\bar{H}$=50	116.56	8	15. 29	0.087			$\bar{H}$=50	111.02	6	22.19	0.059
			$\bar{H}$=500	112.21	10	51.70	0.047			$\bar{H}$=500	111.02	10	68.34	0.059
			$\bar{H}$=1500	112.21	10	124.51	0.047			$\bar{H}$=1500	105.03	10	137.01	0.019
			$\bar{H}$=5000	108.01	10	361.22	0.033			$\bar{H}$=5000	**104.83**	10	381.56	0.001
TD-CITRM_21_3	—	—	$\bar{H}$=10	×	×	×	×	—	—	$\bar{H}$=10	×	×	×	×
			$\bar{H}$=50	125.70	10	58.74	0.095			$\bar{H}$=50	121.86	8	77.26	0.127
			$\bar{H}$=500	122.42	10	93.12	0.067			$\bar{H}$=500	121.86	10	128.08	0.127
			$\bar{H}$=1500	119.92	10	176.05	0.045			$\bar{H}$=1500	115.12	10	225.49	0.065
			$\bar{H}$=5000	**114.71**	10	469.15	0.013			$\bar{H}$=5000	110.30	10	489.03	0.028
TD-CITRM_23_3	—	—	$\bar{H}$=10	×	×	×	×	—	—	$\bar{H}$=10	×	×	×	×
			$\bar{H}$=50	130.71	4	101.13	0.099			$\bar{H}$=50	120.60	3	198.12	0.083
			$\bar{H}$=500	125.42	10	210.62	0.055			$\bar{H}$=500	118.07	10	519.81	0.060
			$\bar{H}$=1500	125.42	10	371.90	0.055			$\bar{H}$=1500	118.07	10	881.44	0.060
			$\bar{H}$=5000	120.83	10	933.24	0.016			$\bar{H}$=5000	115.51	10	1077.3	0.037
TD-CITRM_25_3	—	—	$\bar{H}$=10	×	×	×	×	—	—	$\bar{H}$=10	×	×	×	×
			$\bar{H}$=50	×	×	×	×			$\bar{H}$=50	×	×	×	×
			$\bar{H}$=500	138.72	10	550.11	0.098			$\bar{H}$=500	128.51	10	904.20	0.078
			$\bar{H}$=1500	132.40	10	742.62	0.048			$\bar{H}$=1500	124.10	10	1529.1	0.063

		$\bar{H}$=5000	132.40	10	1519.0	0.033			$\bar{H}$=5000	124.10	10	1994.8	0.041

Acknowledgements:

We thank the Editor and three reviewers for their valuable suggestions and helpful comments which helped us to significantly improve the manuscript.

References

Alinaghian, Mehdi, and Mansoureh Naderipour. "A novel comprehensive macroscopic model for time-dependent vehicle routing problem with multi-alternative graph to reduce fuel consumption: A case study." *Computers & Industrial Engineering* 99 (2016): 210-222.

Androutsopoulos, Konstantinos N., and Konstantinos G. Zografos. "An integrated modelling approach for the bicriterion vehicle routing and scheduling problem with environmental considerations." *Transportation Research Part C: Emerging Technologies* 82 (2017): 180-209.

Behnke, Martin, and Thomas Kirschstein. "The impact of path selection on GHG emissions in city logistics." *Transportation Research Part E: Logistics and Transportation Review* 106 (2017): 320-336.

Bellman, Richard Ernest. "Dynamic programming treatment of the traveling salesman problem." (1961).

Birge, John R., and Francois Louveaux. *Introduction to stochastic programming*. Springer Science & Business Media, (2011).

Bozkaya, Burcin, F. Sibel Salman, and Kaan Telciler. "An adaptive and diversified vehicle routing approach to reducing the security risk of cash-in-transit operations." *Networks* 69.3 (2017): 256-269.

Bula, Gustavo A., H. Murat Afsar, Fabio A. González, Caroline Prodhon, and Nubia Velasco. "Bi-objective vehicle routing problem for hazardous materials transportation." *Journal of cleaner production* 206 (2019): 976-986.

Calvo, R. Wolfler, and Roberto Cordone. "A heuristic approach to the overnight security service problem." *Computers & Operations Research* 30.9 (2003): 1269-1287.

Capgemini Research Institute. World Payments Report 2019. Accessed February 2020. https://www.capgemini.com/es-es/wp-content/uploads/sites/16/2019/09/World-Payments-Report-WPR-2019.pdf

Çimen, Mustafa, and Mehmet Soysal. "Time-dependent green vehicle routing problem with stochastic vehicle speeds: An approximate dynamic programming algorithm." *Transportation Research Part D: Transport and Environment* 54 (2017): 82-98.

Cordeau, Jean-François, and Gilbert Laporte. "The dial-a-ride problem (DARP): Variants, modeling issues and algorithms." *Quarterly Journal of the Belgian, French and Italian Operations Research Societies* 1.2 (2003): 89-101.

Davies, Toby, and Shane D. Johnson. "Examining the relationship between road structure and burglary risk via quantitative network analysis." *Journal of Quantitative Criminology* 31.3 (2015): 481-507.

Donati, Alberto V., Roberto Montemanni, Luca M. Gambardella, and Andrea E. Rizzoli. "Integration of a robust shortest path algorithm with a time dependent vehicle routing model and applications." In *The 3rd International Workshop on Scientific Use of Submarine Cables and Related Technologies,* (2003): pp. 26-31. IEEE, 2003.

Ehmke, Jan Fabian, Ann M. Campbell, and Barrett W. Thomas. "Optimizing for total costs in vehicle routing in urban areas." *Transportation Research Part E: Logistics and Transportation Review* 116 (2018): 242-265.

Ehmke, Jan Fabian, Ann Melissa Campbell, and Barrett W. Thomas. "Vehicle routing to minimize time-dependent emissions in urban areas." *European Journal of Operational Research* 251.2 (2016): 478-494.

Federal Reserve. 2020. Findings from the Diary of Consumer Payment Choice. Accessed September 2020. https://www.frbsf.org/cash/files/2020-findings-from-the-diary-of-consumer-payment-choice-july2020.pdf

Figliozzi, Miguel Andres. "The time dependent vehicle routing problem with time windows: Benchmark problems, an efficient solution algorithm, and solution characteristics." *Transportation Research Part E: Logistics and Transportation Review* 48.3 (2012): 616-636.

Franceschetti, Anna, Emrah Demir, Dorothée Honhon, Tom Van Woensel, Gilbert Laporte, and Mark Stobbe. "A metaheuristic for the time-dependent pollution-routing problem." *European Journal of Operational Research* 259, no. 3 (2017): 972-991.

Funke, Birger, Tore Grünert, and Stefan Irnich. "Local search for vehicle routing and scheduling problems: Review and conceptual integration." *Journal of heuristics* 11.4 (2005): 267-306.

Ghaderi, Abdolsalam, and Robert L. Burdett. "An integrated location and routing approach for transporting hazardous materials in a bi-modal transportation network." *Transportation research part E: logistics and transportation review* 127 (2019): 49-65.

Ghannadpour, Seyed Farid, and Fatemeh Zandiyeh. "A new game-theoretical multi-objective evolutionary approach for cash-in-transit vehicle routing problem with time windows (A Real life Case)." *Applied Soft Computing (2020)*: 106378.

Garaix, Thierry, Christian Artigues, Dominique Feillet, and Didier Josselin. "Vehicle routing problems with alternative paths: An application to on-demand transportation." *European Journal of Operational Research* 204, no. 1 (2010): 62-75.

Gendreau, Michel, Gianpaolo Ghiani, and Emanuela Guerriero. "Time-dependent routing problems: A review." *Computers & operations research* 64 (2015): 189-197.

Gromicho, Joaquim, Jelke J. van Hoorn, Adrianus Leendert Kok, and Johannes MJ Schutten. "Restricted dynamic programming: a flexible framework for solving realistic VRPs." *Computers & operations research* 39, no. 5 (2012): 902-909..

Haghani, Ali, and Soojung Jung. "A dynamic vehicle routing problem with time-dependent travel times." *Computers & operations research* 32.11 (2005): 2959-2986.

Hoogeboom, Maaike, and Wout Dullaert. "Vehicle routing with arrival time diversification." *European Journal of Operational Research* 275, no. 1 (2019): 93-107.

Huang, Yixiao, Lei Zhao, Tom Van Woensel, and Jean-Philippe Gross. "Time-dependent vehicle routing problem with path flexibility." *Transportation Research Part B: Methodological* 95 (2017): 169-195.

Ichoua, Soumia, Michel Gendreau, and Jean-Yves Potvin. "Vehicle dispatching with time-dependent travel times." *European journal of operational research* 144.2 (2003): 379-396.

Jabali, O., T. Woensel, and A. G. de Kok. "Analysis of travel times and CO2 emissions in time-dependent vehicle routing." *Production and Operations Management* 21.6 (2012): 1060-1074.

Krarup, Jakob. "The peripatetic salesman and some related unsolved problems." *Combinatorial programming: methods and applications*. Springer, Dordrecht, (1995): 173-178.

Kumar, Anand, Debjit Roy, Vedat Verter, and Dheeraj Sharma. "Integrated fleet mix and routing decision for hazmat transportation: A developing country perspective." *European Journal of Operational Research* 264, no. 1 (2018): 225-238.

Lai, David SW, Ozgun Caliskan Demirag, and Janny MY Leung. "A tabu search heuristic for the heterogeneous vehicle routing problem on a multigraph." *Transportation Research Part E: Logistics and Transportation Review* 86 (2016): 32-52.

Malandraki, Chryssi, and Mark S. Daskin. "Time dependent vehicle routing problems: formulations, properties and heuristic algorithms." *Transportation science* 26.3 (1992): 185-200.

Malandraki, Chryssi, and Robert B. Dial. "A restricted dynamic programming heuristic algorithm for the time dependent traveling salesman problem." *European Journal of Operational Research* 90, no. 1 (1996): 45-55.

Malandraki, Chryssi. "Time dependent vehicle routing problems: Formulations, solution algorithms and computational experiments." (1989).

Matic, Dragan, Jozef Kratica, and Zoran Maksimovic. "Solving the minimum edge-dilation k-center problem by genetic algorithms." *Computers & Industrial Engineering* 113 (2017): 282-293.

Michallet, Julien, Christian Prins, Lionel Amodeo, Farouk Yalaoui, and Grégoire Vitry. "Multi-start iterated local search for the periodic vehicle routing problem with time windows and time spread constraints on services." *Computers & operations research* 41 (2014): 196-207.

Musah, Anwar, et al. "Assessing the impacts of various street-level characteristics on the burden of urban burglary in Kaduna, Nigeria." *Applied Geography* 114 (2020): 102126.

Ngueveu, Sandra Ulrich, Christian Prins, and Roberto Wolfler Calvo. "Lower and upper bounds for the m-peripatetic vehicle routing problem." *4OR* 8.4 (2010): 387-406.

Park, Yang-Byung. "A solution of the bicriteria vehicle scheduling problems with time and area-dependent travel speeds." *Computers & industrial engineering* 38.1 (2000): 173-187.

Prins, Christian. "Two memetic algorithms for heterogeneous fleet vehicle routing problems." *Engineering Applications of Artificial Intelligence* 22, no. 6 (2009): 916-928.

Qian, Jiani, and Richard Eglese. "Fuel emissions optimization in vehicle routing problems with time-varying speeds." *European Journal of Operational Research* 248.3 (2016): 840-848.

Radojičić, Nina, Aleksandar Djenić, and Miroslav Marić. "Fuzzy GRASP with path relinking for the Risk-constrained Cash-in-Transit Vehicle Routing Problem." *Applied Soft Computing* 72 (2018a): 486-497.

Radojičić, Nina, Miroslav Marić, and Aleksandar Takači. "A New Fuzzy Version of the Risk-constrained Cash-in-Transit Vehicle Routing Problem." *Information Technology and Control*47.2 (2018b): 321-337.

Reinhardt, Line Blander, Mads Kehlet Jepsen, and David Pisinger. "The edge set cost of the vehicle routing problem with time windows." *Transportation Science* 50.2 (2015): 694-707.

Sakip, Siti Rasidah Md, and Anith Nabilah Mustafa. "Street Pattern Identification for Crime Prevention through Environmental Design." *International Journal of Engineering & Technology* 8.1.7 (2019): 246-252.

Setak, M., Z. Shakeri, and A. Patoghi. "A time dependent pollution routing problem in multi-graph." *International Journal of Engineering-Transactions B: Applications* 30.2 (2017): 234-242.

Setak, Mostafa, Majid Habibi, Hossein Karimi, and Mostafa Abedzadeh. "A time-dependent vehicle routing problem in multigraph with FIFO property." *Journal of Manufacturing Systems* 35 (2015): 37-45.

Smith, Lance, and Erin Louis. "Cash in transit armed robbery in Australia." *Trends and issues in crime and criminal justice* 397 (2010): 1.

Soriano, Adria, et al. "The vehicle routing problem with arrival time diversification on a multigraph." *European Journal of Operational Research* (2020).

Soysal, Mehmet, and Mustafa Çimen. "A simulation based restricted dynamic programming approach for the green time dependent vehicle routing problem." *Computers & Operations Research* 88 (2017): 297-305.

Talarico, L., K. Sörensen, and J. Springael. "The risk-constrained cash-in-transit vehicle routing problem with time window constraints." *14th Workshop of the EURO Working Group "EU/ME: the Metaheuristics Community," Hamburg, Germany*. 2013.

Talarico, Luca, Kenneth Sörensen, and Johan Springael. "A biobjective decision model to increase security and reduce travel costs in the cash-in-transit sector." *International Transactions in Operational Research* 24, no. 1-2 (2017a): 59-76.

Talarico, Luca, Johan Springael, Kenneth Sörensen, and Fabio Talarico. "A large neighbourhood metaheuristic for the risk-constrained cash-in-transit vehicle routing problem." *Computers & Operations Research* 78 (2017b): 547-556.

Talarico, Luca, Kenneth Sörensen, and Johan Springael. "Metaheuristics for the risk-constrained cash-in-transit vehicle routing problem." *European Journal of Operational Research*244.2 (2015): 457-470.

Taş, Duygu, Nico Dellaert, Tom van Woensel, and Ton De Kok. "The time-dependent vehicle routing problem with soft time windows and stochastic travel times." *Transportation Research Part C: Emerging Technologies* 48 (2014): 66-83.

Ticha, Hamza Ben, Nabil Absi, Dominique Feillet, and Alain Quilliot. "Empirical analysis for the VRPTW with a multigraph representation for the road network." *Computers & Operations Research* 88 (2017): 103-116.

Ticha, Hamza Ben, Nabil Absi, Dominique Feillet, and Alain Quilliot. "Multigraph modeling and adaptive large neighborhood search for the vehicle routing problem with time windows." *Computers & Operations Research* 104 (2019): 113-126.

Tikani, H., M. Honarvar, and Y. Zare Mehrjerdi. "Developing an integrated hub location and revenue management model considering multi-classes of customers in the airline industry." *Computational and Applied Mathematics* 37, no. 3 (2018): 3334-3364.

Tikani, Hamid, and Mostafa Setak. "Efficient solution algorithms for a time-critical reliable transportation problem in multigraph networks with FIFO property." *Applied Soft Computing* 74 (2019): 504-528.

Tikani, Hamid, Mostafa Setak, and Emrah Demir. "Multi-objective periodic cash transportation problem with path dissimilarity and arrival time variation." *Expert Systems with Applications* (2020a): 114015.

Tikani, Hamid, Reza Ramezanian, Mostafa Setak, and Tom Van Woensel. "Hybrid evolutionary algorithms and Lagrangian relaxation for multi-period star hub median problem considering financial and service quality issues." *Engineering Applications of Artificial Intelligence* 97 (2020b): 104056.

Wen, Liang, and Richard Eglese. "Minimum cost VRP with time-dependent speed data and congestion charge." *Computers & Operations Research* 56 (2015): 41-50.

Xiao, Yiyong, and Abdullah Konak. "The heterogeneous green vehicle routing and scheduling problem with time-varying traffic congestion." *Transportation Research Part E: Logistics and Transportation Review* 88 (2016): 146-166.

Xu, Guoxun, Yanfeng Li, W. Y. Szeto, and Jun Li. "A cash transportation vehicle routing problem with combinations of different cash denominations." *International Transactions in Operational Research* 26, no. 6 (2019): 2179-2198.

Yan, Shangyao, Sin-Siang Wang, and Ming-Wei Wu. "A model with a solution algorithm for the cash transportation vehicle routing and scheduling problem." *Computers & Industrial Engineering* 63, no. 2 (2012): 464-473.

Zhalechian, M., R. Tavakkoli-Moghaddam, B. Zahiri, and M. Mohammadi. "Sustainable design of a closed-loop location-routing-inventory supply chain network under mixed uncertainty." *Transportation Research Part E: Logistics and Transportation Review* 89 (2016): 182-214.

Zhang, Tao, W. Art Chaovalitwongse, and Yuejie Zhang. "Integrated ant colony and tabu search approach for time dependent vehicle routing problems with simultaneous pickup and delivery." *Journal of Combinatorial Optimization* 28.1 (2014): 288-309.